

Rochester Institute of Technology

RIT Digital Institutional Repository

Theses

2016

Extreme Contrast Enchantment of an All-Optical AND Gate

Saif Al Grait
aa6019@rit.edu

Follow this and additional works at: <https://repository.rit.edu/theses>

Recommended Citation

Al Grait, Saif, "Extreme Contrast Enchantment of an All-Optical AND Gate" (2016). Thesis. Rochester Institute of Technology. Accessed from

This Thesis is brought to you for free and open access by the RIT Libraries. For more information, please contact repository@rit.edu.

**Extreme Contrast Enchantment of an All-
Optical AND Gate**

by

Saif Al Grait

Thesis

Submitted in Partial Fulfillment of the Requirements for the Degree of
Master of Science in Telecommunications Engineering Technology

Supervised by

Drew Maywar, Ph.D.

College of Applied Science & Technology

Electrical Computer and Telecommunications Engineering Technology

Rochester Institute of Technology

Rochester, New York

2016

To God:

Praise and thanks to facilitate successes during my life.

To my parents:

I am blissful to grow up under your kindness. Your sacrifices illuminate my life.

To my brothers

I am grateful for your support and nice wishes during my life.

To my wife and sons

Thank you for always being in my side.

To my professors:

Thank you. I appreciate your wonderful help and support.

To my friends:

Thank you all for your very nice encouragement during my study.

"Work is the only thing that gives substance to life."

Albert Einstein

Abstract

Extreme Contrast Enchantment of an All-Optical AND Gate

Saif Al Grait

We experimentally demonstrate a 31.2-dB-contrast all-optical AND gate based on a Fabry-Pérot semiconductor optical amplifier (SOA). Typically, cross phase modulation is the dominant nonlinearity as it shifts a FPSOA resonance to trigger the AND-gate functionality. Cross polarization modulation (XPoIM) is introduced here to produce a distinct output SOP for the high-state power that is different from the low-state power. A linear polarizer is used to block the low-state power to enhance the contrast by 24 dB, far exceeding previous demonstrations for such FPSOA gates.

Acknowledgements

I believe that everything occurs in my life is under God care. My Master's Degree in Telecommunications at Rochester Institute of Technology (RIT) has introduced me to scientific research. It is a great opportunity to work with Prof. Drew Maywar, my research advisor. I am grateful from my deep heart for his support and help during my study. I have to admit that I reached this point of success because of his real support. I learned several skills and experiences from him that will guide my future studying.

Prof. Maywar always advises me to critically focus in my work by setting goals. I will never forget the whiteboard that constantly occupied with his notes, descriptions, and guide points. Prof. Maywar has a wonderful style of education to motivate his students for engaging in research.

I am grateful to Prof. Maywar for his trust for allowing me to conduct my experimental approach in his Photonic Systems Lab. This lab enables me to discover a variety of advanced optical and electric devices. My first peer-reviewed journal is published in Electronics Letters because of his supports. It was a great moment and honors in my life to conduct my research with him. I really got a great opportunity to work with him, and he will always stay in my mental.

To all my Professors, I would like to thank you for your efforts and sharing your great knowledge. It was my honor to be one of your students. Your encouragement has a wonderful role to keep me in the correct path toward better successful goals. I will never forget you. I love you all.

To my family in Iraq, I would like to thank my parents from my deep heart. I am a lucky person because I grow up in lovely family. I will never forget my father words "education is the best tool for your thriving further life". My mother, your kindness and tenderness is the secret behind my successes. I would like to thank my brother and sisters for their motivating and encouraging during my study. I love you.

To my family in Rochester, Thank you for your love and encouragement. My wife, thank you for your for standing in my side during my study and taking care of our sons. My lovely sons, Thank you for your nice smiles. I love you all, and I hope the best for your future. You are always living in my heart.

To all my friends, I am grateful for your nice support and encouragement during my study. Thank you for your nice moments that I spent with you. Please accept my best wishes for your better future.

Table of Contents

1 Introduction.....	1
1.1 Thesis Overview	2
1.2 All optical Signal Processing (AOSP).....	3
1.3 ALL Optical AND gate	4
1.4 Semiconductor Optical Amplifiers (SOAs).....	6
1.4.1 Classification	8
1.4.2 Principles of SOA Amplifications.....	9
1.4.3 Strong Nonlinearities in FPSOA	10
1.5 Polarization of Light	11
1.5.1 Electromagnetic (EM) Energy.....	11
1.5.2 State of Polarization (SOP)	12
1.5.3 Stokes Parameters in Poincare Sphere	13
2 FPSOA Resonance Behavior	20
2.1 Introduction	20
2.2 Longitudinal Modes.....	20
2.3 Longitudinal Modes of the Waveguide	23
2.4 Wavelength Difference between Polarization Mode Resonances	

.....	27
2.5 Resonance Shifts with Injected Current	30
2.6 Resonance Shift with Input power	33
2.7 Resonance shift with Input SOP.....	35
2.8 Optimizing Input Signal to Experience TE Mode.....	39
3 All-Optical AND gate Based on the TE Mode	42
3.1 Introduction.....	42
3.1.1 Principle of Operation.....	42
3.1.2 Optical AND Gate and FPSOA Nonlinearities.....	44
3.2 Experimental Set up	46
3.3 Optical AND Gate Input Signals	48
3.4 Optical AND Gate Polarization	50
3.5 Optical AND Gate Temporal Power.....	52
3.6 Optical AND Gate Spectral Power	54
4 Polarization Rotation during Optical AND Gate	
Operation	57
4.1 Introduction.....	57
4.1.1 Principles of operation	57

4.1.2	Optical AND Gate and Polarization Rotation	58
4.2	Experimental Setup	59
4.2.1	Optical AND gate via Polarization Rotation.....	59
5	Contrast Enhancement of an Optical AND gate	70
5.1	Introduction.....	70
5.1.1	Principle of operation.....	71
5.1.2	The Basic Principle of Output SOP Alignment	71
5.2	Experimental Setup	72
5.2.1	Optical AND gate via output AB SOP Alignment	76
6	Concluding Remarks	80
7	Bibliography	83

List of Tables

1.1	Truth table of an AND gate	4
1.2	Truth table of an AND gate in terms of pulses	5
3.1	Input A with TE mode SOP into the FPSOA	51
3.2	Normalized Stokes parameters of input SOP into FPSOA	51
4.1	Input A SOP via polarization rotation into the FPSOA.....	61
4.2	Normalized stokes parameters of input A SOP	61
4.3	Output AB SOP for the input A=1, B=0 case.....	64
4.4	Normalized output AB SOP for the input A=1, B=0 case.....	64
4.5	Output AB SOP for the input A=1, B=1 case.....	64
4.6	Normalized output AB SOP for the input A=1, B=1 case.....	65

List of Figures

1.1	Schematic diagram of an SOA.....	7
1.2	The two important types of SOAs	8
1.3	Radiation mechanisms in SOA active region	9
1.4	Poincare sphere diagram	18
2.1	Experiment set-up to characterize longitudinal modes of the FPSOA	21
2.2	FPSOA resonance spectrum... ..	22
2.3	Experimental set-up to characterize TE and TM modes of an FPSOA... ..	23
2.4	A basic operation of a linear polarizer to get the polarization modes.....	24
2.5	The TE and TM modes spectrum of the FPSOA	26
2.6	$\Delta = 0$ [-] between TE and TM modes	28
2.7	$\Delta = 0.38$ [-] between TE and TM modes	29
2.8	$\Delta = 0.53$ [-] between TE and TM modes	29
2.9	$\Delta = 0.68$ [-] between TE and TM modes	30
2.10	Gain and refractive index dependence on the carrier density	31
2.11	The carrier density dependence on the drive current value	31
2.12	Resonant modes shift with injected current	32
2.12	Zoom in FP resonances modes	32

2.13	Dependence of the gain and the refractive index on input power.....	33
2.14	Experimental set-up of characterizing the impact of input optical signals on the FPSOA resonances.....	34
2.15	(a) A resonance wavelength shift associated with input power change (b) A resonance peak power involving with changing the input power value	35
2.16	Characterizing ρ value impact on the TE and TM modes shift for fixed value of total input power into the FPSOA.....	37
2.17	Characterizing ρ value impact on the TE and TM resonance peak power	39
2.18	An FPSOA geometry axis.....	40
2.19	Optimizing input SOP to experiences a TE mode	41
3.1	AND gate operation principles	43
3.2	Digital transfer function of an optical AND gate.....	43
3.3	Nonlinearity dependence on carrier density	45
3.4	Optical AND gate experimental setup & truth table.....	46
3.5	Optical AND gate input pulse signals.....	49
3.6	Output AB optical pulse signals of optical AND gate.....	52
3.7	Optical AND gate output AB contrast	53
3.8	Output A signal optimized spectrum	54
3.8	Output AB spectrum contrast of optical AND gate	55

3.9	Optical AND gate spectrum under different signal conditions	56
4.1	Input A SOP manual polarization rotation.....	62
4.2	Optical AND gate output AB undergoing polarization rotation.....	63
4.3	Output AB SOPs on the Poincare sphere.....	65
4.4	(a) Optical AND gate output AB profile accompanied by polarization rotation (b) Output AB SOPs corresponding to output AB oscilloscope trace	66
4.5	Optical AND gate SOA traces under different input conditions	68
5.1	Output AB SOPs alignment for enhancing optical AND gate contrast.....	72
5.2	Experimental set up of an optical AND gate and output AB SOP alignment technique.....	73
5.3	Output AB for input case $A=1, B=0$ before and after introducing the polarizer	76
5.4	Output AB for input case $A=1, B=1$ before and after introducing the polarizer	77
5.5	(a) Optical AB signal having an indiscernible level for solitary A pulse case (b) A contrast of 31.2 dB is measured using the OSA.	78

Chapter 1

Introduction

1.1 Thesis Overview

This thesis aims to utilize the polarization sensitivity of a Fabry-Pérot semiconductor optical amplifier (FPSOA) to enhance the contrast of an optical AND gate. The role of my research is to optimize the injected optical signal conditions like the state of polarization (SOP), input power, and wavelength to optimize the performance of the optical AND gate. The thesis scope provides an analysis of several experimental approaches. These experimental approaches characterize important factors in an FPSOA, for example resonant modes, polarization, and nonlinearities.

In Chapter 2, several experimental results characterize the FPSOA resonant modes. Furthermore, this chapter characterizes the nonlinearity of an FPSOA that introduces the base of the optical signaling processing for optical logic and wavelength conversion. Furthermore, Chapter 2 characterizes transverse electric (TE) and transverse magnetic (TM) modes of an FPSOA.

Chapter 3 investigates the all-optical AND gate by using the interaction between the input pulse signals (TE mode) and a cavity resonance of an FPSOA. This is the basic operation principle of the AND gate, and has been used in previous research.

Chapter 4 investigates the optical AND gate along with polarization rotation. The polarization rotation is achieved by launching the input A pulse signal into the FPSOA TE and TM modes. This is a new study has not been researched before.

In Chapter 5, a new technique is used to control the output AB SOP to enhance the contrast of the optical AND gate. This technique realizes a 31.2 dB contrast of the optical AND gate that far exceeds previous research.

Chapter 6 is the conclusion of my thesis. The remaining sections of Chapter 1 will briefly describe several fields that intersect with my research. Readers familiar with thesis subjects may skip directly to Chapter 2.

1.2 All-Optical Signal Processing (AOSP)

Deploying optical communication systems has exponentially increased worldwide. Users seek the high-speed transmission of optical systems to utilize high capacity of reliable data communications [1]. Optical signals would require signal processing for equalization, regeneration, amplification, switching, and distributing during transmission due to several purposes [1], for example regeneration and amplification to compensate the distortion and attenuation impairments respectively. This trend toward high-speed optical systems motivates researchers to work on all-optical signal processing [1].

Although the electrical domain has been widely used to process optical signals, the important reason of interest toward AOSP is to eliminate the need of converting the signals from the optical-to-electrical-to-optical (OEO) domain [1, 2]. All-optical signal processing has the potential advantage to process optical signals in the optical domain, which reduces the latency time of traveling optical signals in the transmission line nodes [2]. Another important reason of AOSP is to reduce the complexity of OEO conversion [1, 2].

Both optics and electronics have advantages and disadvantages for signal processing, but optics is more reliable and efficient to process a signal if it is already in the optical domain [1]. For example if optical signals require wavelength conversion to change the transmitted wavelength channel, this conversion requires OEO conversion to achieve this conversion in the absence of using AOSP. Thus, AOSP can achieve this conversion in the optical domain to avoid OEO disadvantages. AOSP eliminates the delay process of OEO conversion [2].

Furthermore, optical signal processing provides THz bandwidth of processing by taking advantage of ultrafast nonlinear optics [2]. Another advantage of using AOSP is to avoid the usage of expensive OEO conversion devices, power consumption, and errors during the conversion process [2]. Consequently, all-optical signal processing may improve the efficiency of the optical systems with less cost, power consumption, and high speed by minimizing the need of OEO conversion in the line of the optical communication systems.

1.3 All Optical AND Gate

AOSP has become an important tool to perform optical-processing functions such as a basic gate, comparator, full adder, and ultrafast control and switching operations [2]. Nonlinear phenomena have a significant role to realize all-optical signal processing. Such phenomena include nonlinear polarization rotation (NPR), cross phase modulation (XPM), and cross gain modulation (XGM) [2]. These phenomena support several advanced optical processing applications like wavelength conversion and optical logic gates [3, 4].

The optical AND gate is one of the significant functional applications of AOSP that has been demonstrated in previous research [3, 4]. This thesis aims to demonstrate an optical AND gate based on the resonance cavity of an FPSOA [3]. An all optical AND gate is a basic combinational logic gate for optical signals. In the combinational mechanism, the output is a consequence of the present input signals. The basic output operation of an optical AND gate is illustrated in truth Table 1.1.

Input A	Input B	Output AB
0	0	0
1	0	0
0	1	0
1	1	1

Table 1.1: Truth table of an AND gate.

Table 1.1 shows the basic functionality of an optical AND gate. The basic logic AND gate consists from two input signals (input A and input B) in the left side of the table. The right side of the table represents the output AB of an optical AND gate. The binary number one (1) in the truth table indicates a high state power of a signal while the binary number zero (0) indicates a low state power of a signal. The output AB of an AND gate is high if both input A and input B have high power values. In addition, the output AB is low power if at least one of the input signals is low power.

Input A	Input B	Output AB
0	0	Low00
Pulse	0	Low10
0	Pulse	Low01
Pulse	Pulse	High

Table 1.2: Truth table of an AND gate in terms of pulses.

Table 1.2 represents the truth table of an optical AND gate in terms of pulses. Input A and input B are two input optical pulses. My research objective is to optimize the output AB power for the case dual input A and input B optical pulses injected together into the FPSOA cavity. In addition, a research objective of my thesis is to minimize the output AB power for the remaining cases such as, solitary input-A case (A= 1, B= 0) injected into the FPSOA cavity. The contrast is measured by calculating how much the output AB high case is higher than the remaining output AB low cases in the truth table 1.2. This results in three contrast values:

$$\begin{aligned}
 \text{Contrast } 00 &= \frac{\text{High}}{\text{Low } 00}, \\
 \text{Contrast } 10 &= \frac{\text{High}}{\text{Low } 10}, \\
 \text{Contrast } 01 &= \frac{\text{High}}{\text{Low } 01}.
 \end{aligned}
 \tag{1.1}$$

The optical AND gate benefits from an interaction between the input pulses and the FPSOA cavity resonance to achieve a high contrast enhancement. Optical AND gate contrast enhancement requires controlling independent parameters such as input power, wavelength, and the state of polarization (SOP) of the input A and input

B pulses. Furthermore, controlling these independent signal parameters is necessary to obtain specific behavior of FPSOA quantities such as resonance cavities, carrier density, refractive index, and gain.

Although controlling the input signal conditions before an FPSOA is necessary to conduct an optical AND gate experiment, this thesis also uses a recent technique [5] to control the output AB optical AND gate SOPs. Controlling the optical AND gate input SOPs is achieved by cross polarization modulation (XPolM). XPolM is optimized to produce a distinct SOP for the high state power that is different from the SOP for the low state power; a linear polarizer is placed after an FPSOA to block the low state power ($A= 1, B= 0$) while this polarizer allows the high state power ($A= 1, B= 1$) to partially pass through it. This technique demonstrated a 31.2 dB optical AND gate. This contrast exceeds the previous demonstrated data by over 24 dB.

1.4 Semiconductor Optical Amplifiers (SOAs)

Although semiconductor optical amplifiers (SOAs) have been widely used as booster amplifiers, in line amplifiers, and preamplifiers in optical communication systems [7], SOAs have become important devices to realize a variety of optical functional applications [7]. AOSP is the most typical functional application, such as optical switching, memory, signal-regeneration, wavelength conversion [6], optical flip-flop operation [5], and optical AND gate operation [3, 4]. SOAs have become an attractive system for AOSP because they support operation of low injected optical powers with strong optical nonlinearities [6].

Figure 1 shows the schematic diagram of an SOA. An SOA has an active region and waveguide. The SOA amplifies the input optical signal when it passes through the active region of the waveguide [7].

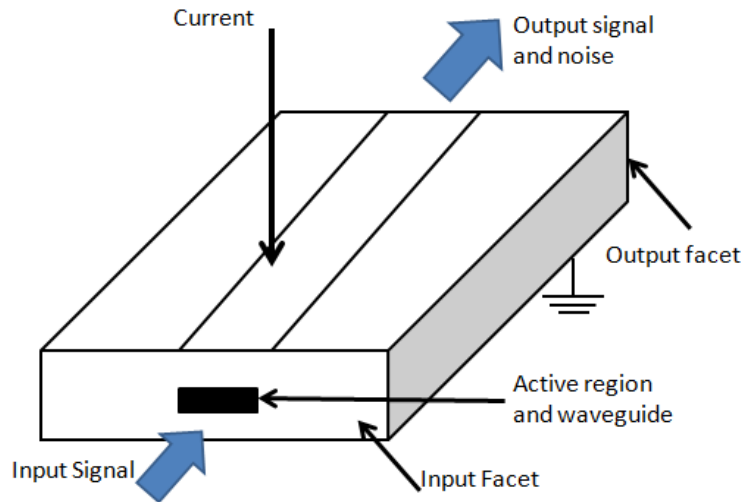


Figure 1.1: Schematic diagram of an SOA.

An input optical signal enters the SOA waveguide through the input facet. The SOA waveguide confines the input signals inside the active region in the direction of propagation. An external laser diode controller provides an external drive current. The drive current provides carriers (electrons) inside the active region [7]. The amplified output optical signal leaves the SOA waveguide through the output facet. The process of amplification produces unavoidable optical noise that cannot be eliminated. This optical noise is called amplified spontaneous emission (ASE) [7, 8]. Although SOAs have wideband optical noise, SOAs support strong nonlinear effects that enable them to become an important tool in photonic integrated circuits (PICs) and AOSP [8].

1.4.1 SOA Classification

There are two substantial types of SOAs as shown in Figure 2. These two types can be classified according to their gain spectrum.

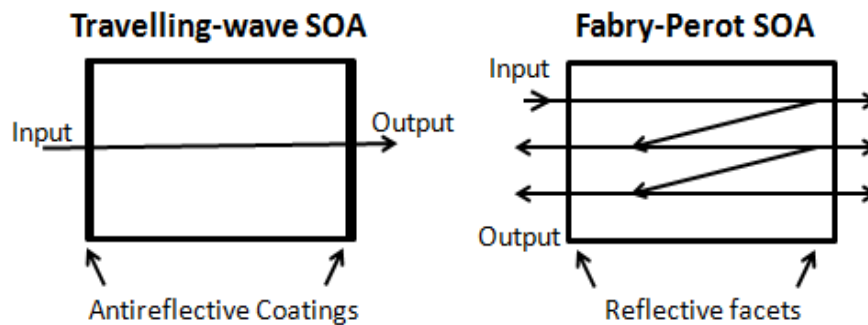


Figure 1.2: The two important types of SOAs.

The first type is the travelling-wave SOA (TWSOA). In this type, the end facets do not provide reflection by using anti-reflection coatings with reflectivity $< 10^{-5}$ [7, 8]. Thus, the light wave has the opportunity of amplification by only one pass through the waveguide. Because it has anti-reflection coating, the TWSOA provides a smooth gain spectrum [7].

The second type is the resonant type Fabry-Pérot SOA (FPSOA). In this type, the optical signals reflect back and forth from the end facets of the FPSOA. These reflection end facets enable several bounces back and forth of injected light inside the FPSOA so that the light can experience more optical gain at certain wavelengths [8]. Furthermore, the gain spectrum of an FPSAO has ripples due to the end facets [7].

1.4.2 Principles of SOA Applications

The active region has two important electronic energy bands; the energy bands are the conduction band (CB), and the valence band (VB) [8]. The external injection current into the active region provides charge carriers inside the FPSOA. These carriers occupy energy states in the CB and leave holes in the VB [8]. Three processes may happen when a light signal propagates into the FPSOA active region as shown in Figure 3.

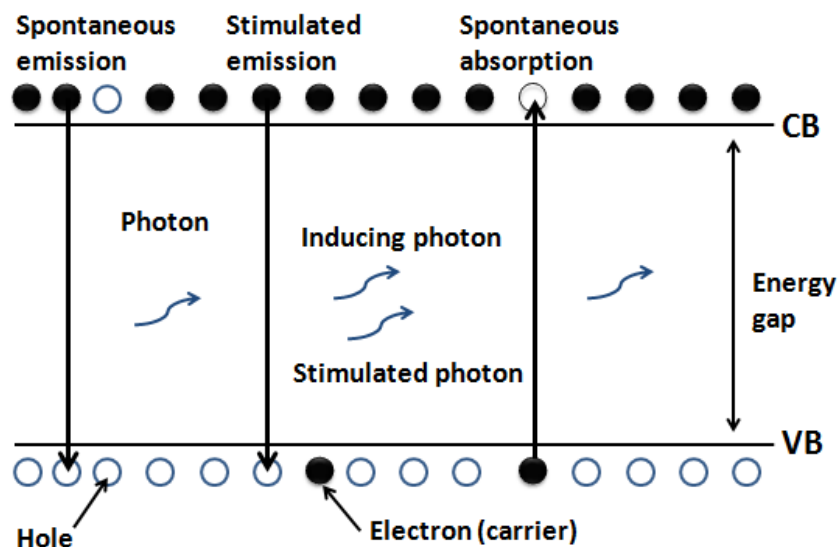


Figure 1.3: Radiation mechanisms in an SOA active region.

These three processes are referred to as radiation mechanisms [7]-[8]. The first radiation mechanism is stimulated emission. In this process, a charge carrier travels from the CB to the VB. This stimulated photon will acquire the same physical specifications of the incident photon, like phase, frequency, and direction. Thus, this process is responsible for providing optical gain that amplifies the injected optical signals into the FPSOA [7]-[8]. Therefore, this is a desired radiation mechanism.

The second radiation mechanism is stimulated absorption. This process happens if a carrier travels from the VB to the CB, which extinguishes the incident photon. The last radiation mechanism is spontaneous emission. This process produces wide band optical noise. This process happens if a carrier travels from the CB to the VB due to uncontrolled conditions resulting in a random phase with a wide range of frequencies.

1.4.3 Strong Nonlinearities in FPSOAs

The FPSOA has become an important device for optical bistability and switching applications due to its strong nonlinearity [10]. Cross phase modulation (XPM), cross gain modulation (XGM), and cross polarization modulation (XPoLM) have become important nonlinear mechanisms to conduct a wide number of AOSP applications [10]. The general concept of these nonlinear phenomena is the nonlinear interaction of two sources to produce change in polarization state, power, and phase.

XPM means that phase changes according to refractive index changes due to another optical signal inside the nonlinear medium. XPM is associated with self phase modulation (SPM). SPM is a nonlinear effect that changes the phase of light signals according to the changing in the refractive index of the nonlinear medium. This thesis uses the nonlinear interaction between the input AND gate pulse signals and a cavity resonance of an FPSOA. XPM, XGM, and XPoLM phenomena are utilized to achieve high contrast of the optical AND gate.

1.5 Polarization of Light

1.5.1 Electromagnetic (EM) Energy

A lightwave is electromagnetic (EM) energy. Optical communication systems use electromagnetic (EM) waves to transmit and receive optical signals via optical waveguides [11]. Electromagnetic (EM) waves consist of two orthogonal electrical field and magnetic field vectors that point perpendicular to the direction of propagation [11]. Thus, a lightwave is a transverse electromagnetic wave that vibrates perpendicularly to the direction of the propagation. The variation of a transverse electromagnetic wave with time defines the state of polarization (SOP). The polarization is a fundamental property of a lightwave [11].

Each field of a polarized wave is the composition of two orthogonal SOPs. These two orthogonal SOPs can be defined as a transverse electric (TE) and transverse magnetic (TM) according to the structure of consideration [13]. The polarized light is decomposed in linear horizontal polarized (LHP) light and linear vertical polarized light (LVP). For our research, the LHP is the TE mode, and the LVP is the TM mode. Equation 1.2 shows that the total optical power is the sum of the power of the TE and TM modes.

$$P_{\text{polarized}} = P_{\text{TE}} + P_{\text{TM}}. \quad 1.2$$

In this thesis, controlling the SOP of an optical signal enhances the contrast of an optical AND gate due to the polarization sensitivity of an FPSOA cavity resonance. Many optical devices in this research study are extremely sensitive to the polarization state, like the Mach-Zehnder Modulator (MZM), polarizer, and FPSOA.

These devices require a specific SOP to achieve a particular behavior. An MZM requires an SOP oriented to its planar waveguide to operate appropriately. A polarizer is an optical device that allows only one polarization component to pass through it and blocks the other. An FPSOA is a polarization dependent device that gives an output power that depends on the input SOP.

In this research, an FPSOA is polarization dependent; polarization dependent means that the TE and TM modes of an FPSOA exhibit different amount of nonlinear phenomena like XPM and XGM when light waves are injected into the FPSOA [13]. The FPSOA is also birefringent, which means a different refractive index is experienced for TE and TM modes in the resonance cavity. In addition, an FPSOA is asymmetric in gain; an FPSOA has a higher gain profile for the TE mode than the TM mode. Moreover, the line-width enhancement factor is different between modes due to different physical geometry. The line-width enhancement factor measures the ratio of phase and gain change for each mode in an FPSOA.

1.5.2 State of Polarization (SOP)

Light waves can have one of a variety of state of polarizations (SOPs). For example, the SOP of a light wave may be a linear, circular, and elliptical polarization. Light waves may also have an SOP that varies randomly in time; these light waves are unpolarized light [12, 13]. The total power of an optical signal is the combination of polarized and unpolarized light as shown in equation 1.3.

$$P_{\text{total}} = P_{\text{unpolarized}} + P_{\text{polarized}} \quad 1.3$$

Equation 1.3 illustrates that the total power consists of unpolarized SOP and polarized SOP for an optical signal. A degree of polarization (DOP) is an expression to find the amount of polarized light from the total power of an optical signal. The DOP has values from zero (unpolarized light) to one (completely polarized light). The DOP is defined as the ratio of polarized light to the total power of an optical signal as in equation 1.4:

$$\text{DOP} = \frac{P_{\text{polarized}}}{P_{\text{total}}} = \frac{P_{\text{TE}} + P_{\text{TM}}}{P_{\text{unpolarized}} + P_{\text{TE}} + P_{\text{TM}}}. \quad 1.4$$

1.5.3 Stokes Parameters & Poincare Sphere

The polarimeter is an optical diagnostic tool. This device measures the SOP and degree of polarization (DOP) of optical signals. This device is important in several series of experimental work in this research. The aim of using the polarimeter is to measure, set, and optimize the polarization property of light waves in this research.

The polarimeter uses four Stokes parameters to characterize optical signals. The Stokes parameters are defined as (S_0, S_1, S_2, S_3) . Each parameter has a physical meaning to interpret the polarization of optical signals. The S_0 Stoke parameter represents the total power (polarized and unpolarized light):

$$S_0 = P_{\text{unpolarized}} + P_{\text{polarized}}. \quad 1.5$$

$$S_0 = P_{TE} + P_{TM} + P_{\text{unpolarized}} \quad 1.6$$

The S_1 Stokes parameter measures the difference between the LHP and the LVP. For example, if S_1 is bigger than zero, LHP is more than LVP:

$$S_1 = P_{TE} - P_{TM} \quad 1.7$$

The S_2 Stokes parameter is the difference between linear polarization along the 45- and 135-degree axes:

$$S_2 = P_{45} - P_{135} \quad 1.8$$

The S_3 Stokes parameter is the difference between right-handed circular polarization (RCP) and left-handed circular polarization (LCP):

$$S_3 = P_{RCP} - P_{LCP} \quad 1.9$$

Stokes parameters S_1 , S_2 , S_3 are used to present a unique point on the Poincare sphere where the set of Stokes parameters is a 3D vector. Stokes parameters S_1 , S_2 , S_3

are utilized to construct the Poincare sphere. The state of polarization (SOP) is represented by a unique point the Poincare sphere. The magnitude of the Poincare vector is given by:

$$|S| = \sqrt{S_1^2 + S_2^2 + S_3^2}. \quad 1.10$$

This magnitude is equal to the total polarized power $P_{\text{polarized}}$ as in equation 1.11:

$$P_{\text{polarized}} = \sqrt{S_1^2 + S_2^2 + S_3^2}. \quad 1.11$$

Recalling equation 1.4, the DOP can be written in terms of the Stokes parameters as:

$$\text{DOP} = \frac{P_{\text{polarized}}}{P_{\text{total}}} = \frac{\sqrt{S_1^2 + S_2^2 + S_3^2}}{S_0} \quad 1.12$$

The Stokes parameters (S_1, S_2, S_3) can be normalized by the total power (S_0) in order to limit the magnitude of the Stokes vector to unity. The normalized Stokes parameters with total power are:

$$\delta_1 = \frac{S_1}{S_0}. \quad 1.13$$

$$\delta_2 = \frac{S_3}{S_0}. \quad 1.14$$

$$\delta_3 = \frac{S_3}{S_0}. \quad 1.15$$

Using these normalized quantities, the DOP may now be written as:

$$DOP = \frac{\sqrt{S_1^2 + S_2^2 + S_3^2}}{S_0}. \quad 1.16$$

$$DOP = \sqrt{\frac{S_1^2}{S_0^2} + \frac{S_2^2}{S_0^2} + \frac{S_3^2}{S_0^2}}. \quad 1.17$$

$$DOP = \sqrt{\delta_1^2 + \delta_2^2 + \delta_3^2}. \quad 1.18$$

Thus, the length of the vector $(\delta_1, \delta_2, \delta_3)$ is the DOP:

$$|S| = \sqrt{\delta_1^2 + \delta_2^2 + \delta_3^2} = DOP. \quad 1.19$$

One final normalization scheme can force the point of the Poincare vector to be on the surface of the unit sphere. The process of normalization is obtaining by dividing the normalized Stokes parameters $\delta_1, \delta_2, \delta_3$ by their DOP value.

$$s_1 = \frac{\delta_1}{\text{DOP}}. \quad 1.20$$

$$s_1 = \frac{S_1 S_0}{S_0 \sqrt{S_1^2 + S_2^2 + S_3^2}} = \frac{S_1}{\sqrt{S_1^2 + S_2^2 + S_3^2}} = \frac{S_1}{|S|}. \quad 1.21$$

$$s_2 = \frac{\delta_2}{\text{DOP}}. \quad 1.22$$

$$s_2 = \frac{S_2 S_0}{S_0 \sqrt{S_1^2 + S_2^2 + S_3^2}} = \frac{S_2}{\sqrt{S_1^2 + S_2^2 + S_3^2}} = \frac{S_2}{|S|}. \quad 1.23$$

$$s_3 = \frac{\delta_3}{\text{DOP}}. \quad 1.24$$

$$s_3 = \frac{S_3 S_0}{S_0 \sqrt{S_1^2 + S_2^2 + S_3^2}} = \frac{S_3}{\sqrt{S_1^2 + S_2^2 + S_3^2}} = \frac{S_3}{|S|}. \quad 1.25$$

Note that this normalization scheme is just the original Stokes parameters normalized by the total polarized power.

the length of the vector (s_1, s_2, s_3) is unity:

$$|s| = \sqrt{s_1^2 + s_2^2 + s_3^2}, \quad 1.26$$

$$|S| = \sqrt{\frac{S_1^2}{|S|^2} + \frac{S_2^2}{|S|^2} + \frac{S_3^2}{|S|^2}}, \quad 1.27$$

$$|S| = \frac{\sqrt{S_1^2 + S_2^2 + S_3^2}}{|S|} = \frac{|S|}{|S|} = 1. \quad 1.28$$

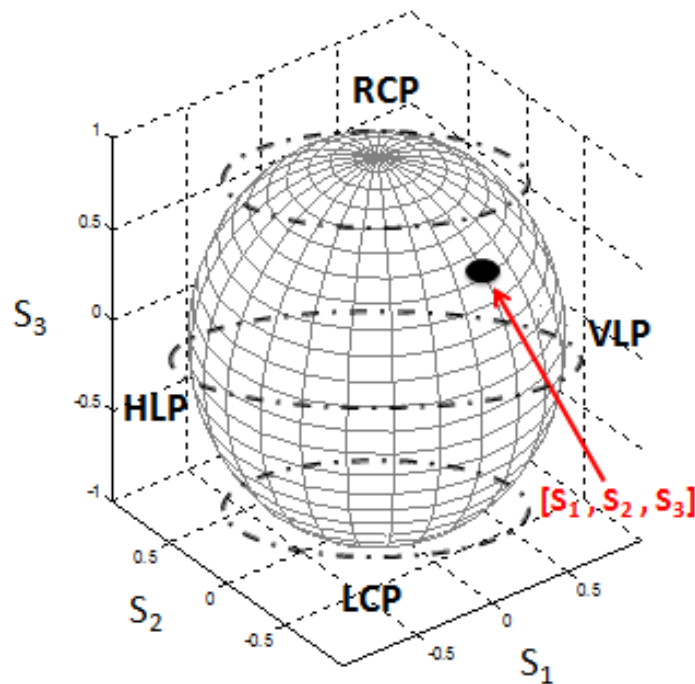


figure 1.4: Poincare sphere diagram.

Figure 1.4 shows a unique point on the Poincare sphere. This sphere characterizes the shape of specific pattern of an optical signal according to the location of this point on the sphere. A specific pattern shape represents the state of polarization (SOP) of an optical signal. For example,

- A point on the top pole of the Poincare sphere has a RCP SOP with Stokes parameters of $(0, 0, 1)$.
- A point on the bottom pole of the Poincare has a LCP SOP with Stokes parameters of $(0, 0, -1)$.
- A point on the equator of the Poincare sphere has a HLP or VLP with coordinates $(1, 0, 0)$ and $(-1, 0, 0)$ respectively.
- Any other points between the poles and equator are considered as elliptical SOP.

Chapter 2

FPSOA Resonance Behavior

2.1 Introduction

This chapter characterizes FPSOA resonances (or longitudinal modes) under several experimental conditions, for example, a change in carrier density of the active region. Furthermore, this chapter studies the birefringence of an FPSOA. The goal of this investigation is to study the relationship between the carrier density and resonances with different power, wavelength, and state of polarization (SOP) of injected optical signals into an FPSOA. Characterizing resonances of an FPSOA provides important knowledge for investigating optical AND gates later in this thesis.

2.2 Longitudinal Modes

An FPSOA is a resonant type of SOA. FPSOAs have two side reflections. When optical signals enter into the FPSOA active region, they will bounce back and forth between the two reflective facets. This bouncing back and forth will enable the injected light to gain more photons. The resonant cavity of an FPSOA allows only wavelengths of a standing wave pattern to experience constructive interference (CI) while other wavelengths are subjected to experience destructive interference (DI). This broadband interference pattern of the FPSOA can be seen clearly with amplified spontaneous emission (ASE).

Figure 2.1 shows the experimental set-up to characterize the FPSOA resonant cavity without injecting optical signals into the FPSOA. The laser controller (LC- ILX Lightwave LDC- 3908) provides the external drive current to the active region of the FPSOA. The driving current set to 62 mA at temperature of a 20 C°. The dotted line is an RS-232 electrical cable that connects the LC with the FPSOA. The optical spectrum analyzer (OSA- Yokogawa AQ630B) captures the output power of the FPSOA. The solid line is a signal mode fiber that connects the output of the FPSOA into the OSA diagnostic.

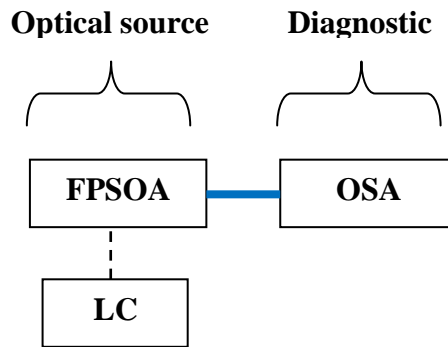


Figure 2.1: Experiment set-up to characterize longitudinal modes of the FPSOA

Figure 2.2 shows the ASE spectrum is the OSA trace that indicates the presence of the longitudinal modes of the FPSOA. This figure shows a one-nm range of the wavelength spectrum in the x-axis. This wavelength spectrum shows as a constructive interference (strong peak power) and a destructive interface (low peak power) in the OSA trace. Longitudinal modes are formed at discrete wavelengths that correspond to an integer number of the cavity resonance.

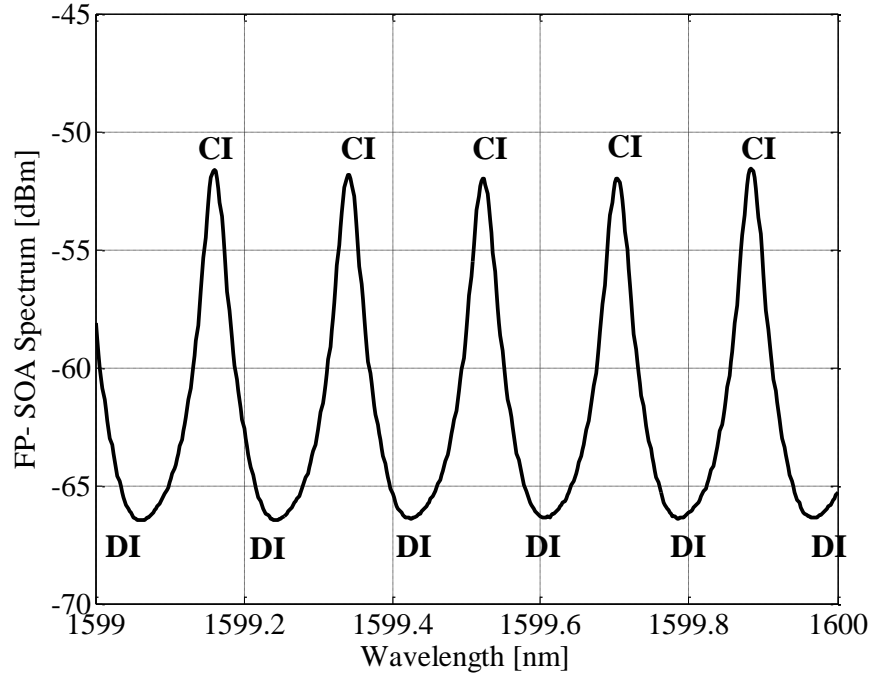


Figure 2.2: FPSOA resonant spectrum

Figure 2.2 shows resonances that experience constructive interference (CI) and anti-resonances that experience destructive interference (DI). This process of having longitudinal modes depends on the waveguide length (L) that determines the round trip of the input signal to reflect between the end facets of the FPSOA [7]. The distance of round trip is $(2L)$. In addition, a standing wave occurring is associated with refractive index (n) of the waveguide medium, and free-space wavelength (λ_0) values in the active region [7]. Equation 2.1 explains the relationship between these parameters.

$$m = \frac{2nL}{\lambda_0}. \quad 2.1$$

2.3 Longitudinal Modes of the Waveguide

Characterizing the transverse electric (TE) and transverse magnetic (TM) modes of an FPSOA is an important subject in this thesis. This characterization is necessary to understand the polarization dependence of an FPSOA. The main two important investigated factors are the power strength of each mode and the central wavelengths differences between TE and TM modes (Δ). The gain of an FPSOA is different between the TE mode the TM mode due to several factor. This means the ratio of peak to valley power of TE mode is different from the ratio for the TM mode.

Figure 2.3 shows the experimental set-up to decompose output optical signals from the FPSOA into the TE and the TM modes; this process requires polarization controllers (PCs), a polarization beam splitter (PBS), and a polarimeter (POD).

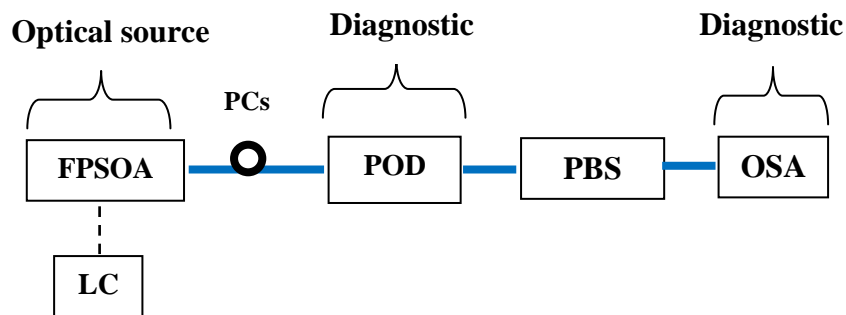


Figure 2.3: Experimental set-up to characterize TE and TM modes of an FPSOA.

Figure 2.3 shows that the LC connected with the FPSOA by an RS-232 electrical cable. Single mode fibers connect between the FPSOA, POD, PBS, PC, and the OSA. The polarizer passes the TE or TM modes through its output port and blocks the other respectively. The polarimeter (POD- 101D from General Photonics) with 100 KHz bandwidth was used to measure Stokes parameters for each mode, which provides the state of polarization (SOP) and degree of polarization (DOP). The SOA

is an essential diagnostic to get the polarization modes of the FPSOA due to the high sensitivity of tracking low optical powers of this device. Furthermore, this device was used to capture the spectrum of the polarization modes.

Figure 2.4 shows a basic schematic diagram that explains the basic process of separating the polarization modes of the FPSOA.

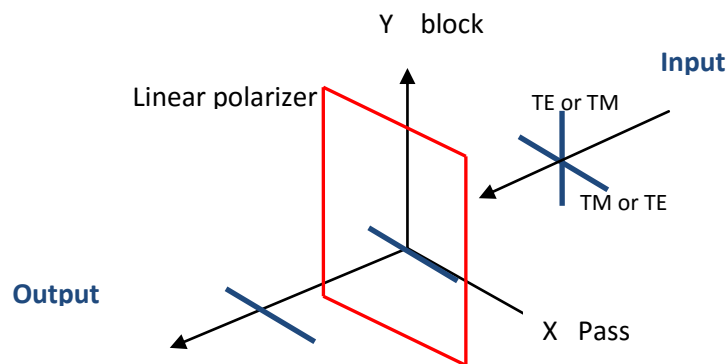


Figure 2.4: A basic operation of a linear polarizer to get the polarization modes

This figure explains the role of the polarizer to allow only the TE or TM mode to pass through it when the SOP orientation of the TE or TM mode is aligned in parallel to the passing x-axis of the polarizer and perpendicular to the direction of propagation. Because the polarization modes are orthogonal to each other in the propagation direction, solitary the TE or TM mode can pass through the x-axis of the polarizer.

The experimental procedures of obtaining the TE and TM modes are given below:

- After connecting the experimental set-up as in Figure 2.3, set the LC to provide an external drive current of $I = 62 \text{ mA}$ (2.1 mA below the lasing threshold) at temperature of $T = 20 \text{ C}^\circ$ into the active region of the FPSOA.

- The first step is setting the OSA functions to track the output FPSOA resonances. a) Set the OSA resolution to 0.02 nm, b) Set the OSA span function to one or two nm (zooming in specific region of the FPSOA spectrum), c) Set the OSA to experience a high sensitivity mode, and d) set the OSA sweep function on repeat mode.
- The second step is working on obtaining the TM spectrum. Because the FPSOA waveguide provides less gain for TM mode, this mode has a minimum peak to valley height.
- The PCs placed after the FPSOA were used to align the FPSOA output SOP. This process requires slowly changing the PCs until only TM mode pass the through the passing x-axis of the polarizer. Then, the OSA was used to capture the TM spectrum, and the polarimeter was used to measure the values of Stokes parameters.
- The third step is re-changing PCs after the FPSOA to get the TE mode in the OSA trace. TE mode has a higher ratio of the peak to valley height than TM mode in FPSOA.
- Obtaining the TE mode means forcing this mode to be in parallel to the pass x-axis of the polarizer while the TM mode is blocked by the polarizer. Then, the OSA was used to capture the TE spectrum, and the polarimeter was used to measure the values of Stokes parameters.

Figure 2.5 shows the spectrum results for the TE and TM modes in the OSA trace with a wide spectrum of 75 nm. This figure shows the spectral range from 1550 nm to 1625 nm.

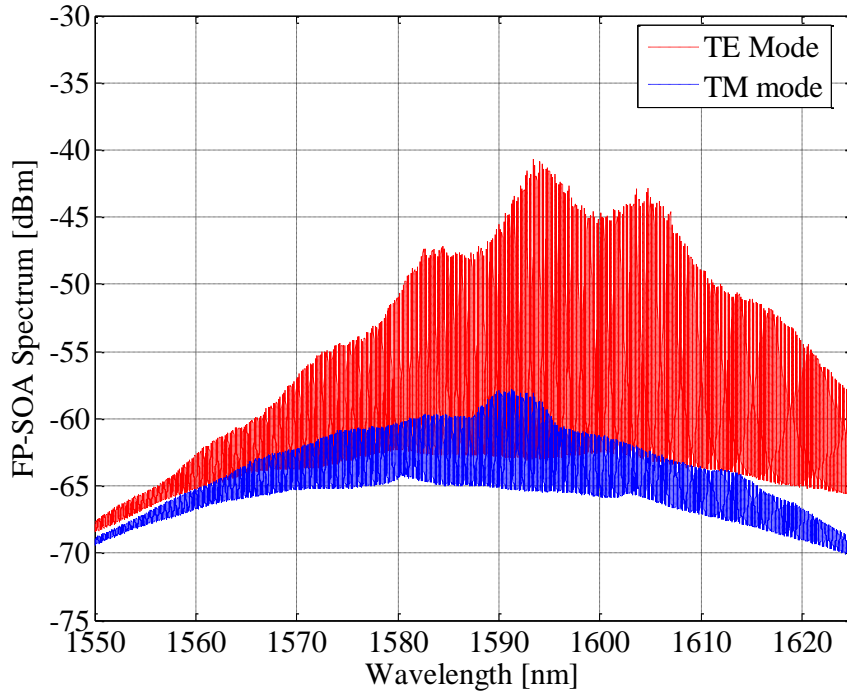


Figure 2.5: the TE and TM modes spectrum of the FPSOA

The spectrum shows that the TE mode has highest ratio of peak to valley height than the TM mode as expected due to anisotropic gain. The FPSOA has an anisotropic gain in part because the confinement factor for TE mode is different from TM mode due to the waveguide geometry.

Furthermore, this figure shows that the TM mode valley power has a lower value than TE valley power in the OSA trace. The reason behind that might be associated with polarization dependent loss (PDL) impairment that influences differently on the polarization modes in a single mode fiber (SMF); SMF connects between the polarizer and the OSA.

In summary, the process of the obtaining the polarization modes of the FPSOA requires adding PCs and a linear polarizer after the FPSOA. The PCs help to orient the TE or TM mode to the passing x-axis of the polarizer to obtain each mode separately in the OSA trace.

2.4 Wavelength Difference between Polarization Mode Resonances

An FPSOA is a birefringent device; this device has a different refractive index for the TE and TM modes. This experiment characterizes the FPSOA refractive index variations between TE and TM modes (FPSOA birefringence). The process of characterizing FPSOA birefringence is achieved by following the experimental procedures of obtaining TE and TM modes outlined in Section 2.3.

The procedure of obtaining a wavelength difference Δ between the TE and TM mode requires zooming into a short range of resonances wavelengths. The OSA span setting can help to set the starting wavelength, ending wavelength, and span value to track specific resonances of the FPSOA. Equation 2.2 shows the mathematical calculation of finding the normalized wavelength difference $\Delta [-]$:

$$\Delta [-] = \frac{(\lambda_{TM} - \lambda_{TE}) [\text{nm}]}{0.18 [\text{nm}]} . \quad 2.2$$

The λ_{TM} is the wavelength of TM resonance, and λ_{TE} is the wavelength of TE resonance. The number 0.18 nm is the wavelength difference between any two TE or TM resonances. The 0.18 nm number is used to normalize the wavelength difference $\Delta [-]$ between zero to one. When the Δ value equals to 0 or 1 [-], both the TE and TM resonances are in phase. Moreover, when Δ equals to 0.5 [-], the TE and TM resonances are out of phase.

Figure 2.6 shows that the TE and TM modes are in phase for $\Delta = 0$ [-]. This figure shows that both modes have the same central wavelength of interference pattern.

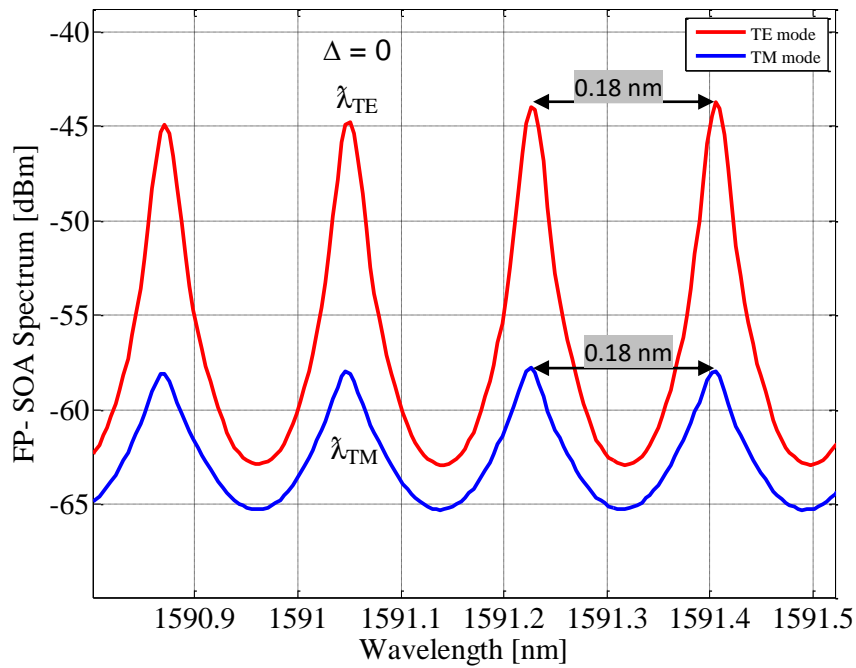


Figure 2.6: $\Delta = 0$ [-] between TE and TM modes

Figure 2.7 shows a wavelength difference $\Delta = 0.38$ [-] between TE and TM modes. This figure shows a partial power of TE mode still shown with the TM mode resonance. The reason of this inefficient separation is because the OSA settings were allocated to find TE and TM modes for $\Delta = 0$ [-] and not for $\Delta = 0.38$ in Figure 2.7.

These experimental results show that it is impossible to fully separate the TE and TM modes for a wide span of 75 nm. To totally separated between the TE and TM modes, one needs to focus on a short range of spectrum in the OSA trace (around one or two nanometer) for each assigned wavelength region.

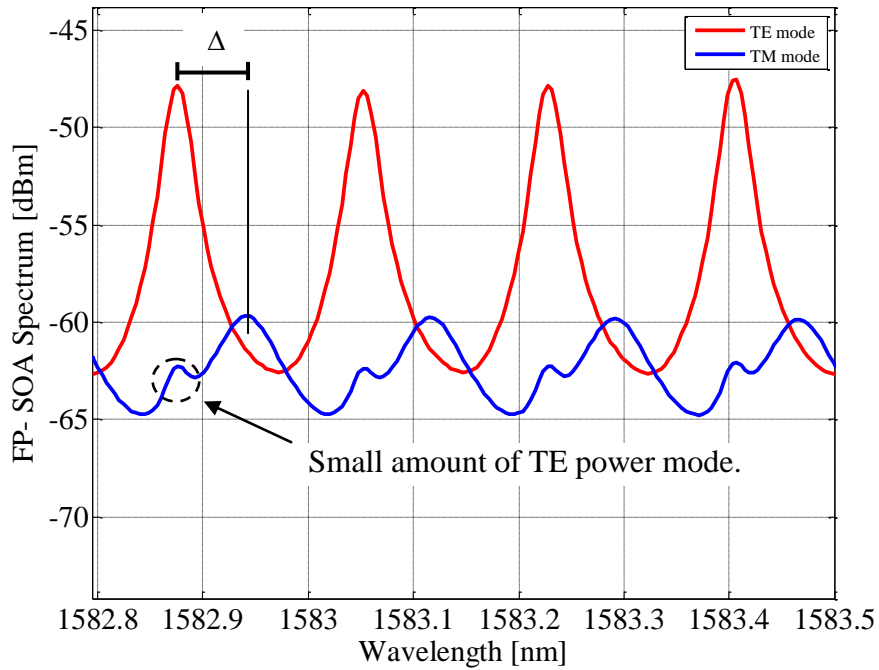


Figure 2.7: $\Delta = 0.38$ [-] between TE and TM modes

Figure 2.8 shows another value of $\Delta = 0.53$ [-] between the two polarization modes. In this Δ value, the TE and TM modes are out of phase.

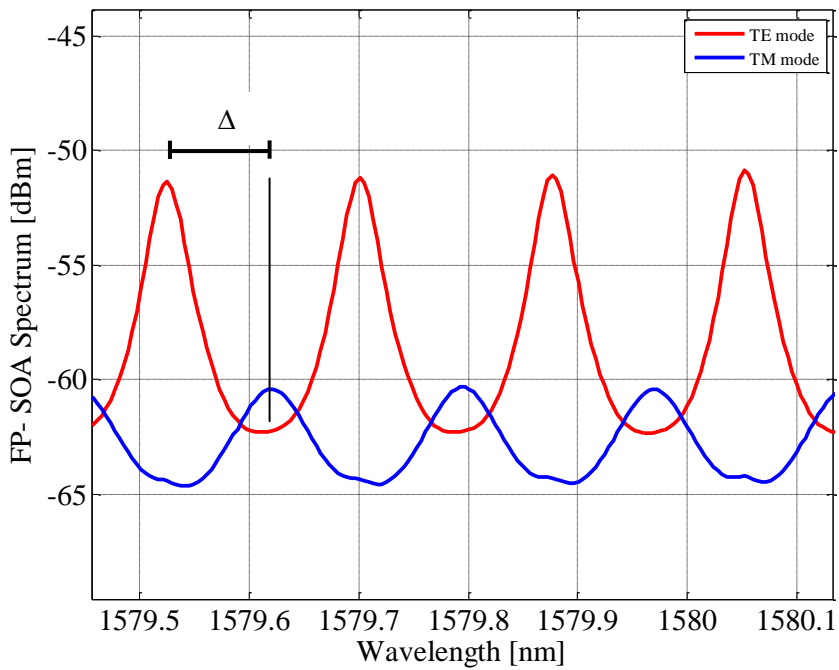


Figure 2.8 $\Delta = 0.53$ [-] between TE and TM modes

Figure 2.9 shows $\Delta = 0.68$ [-] between the TE and TM modes.

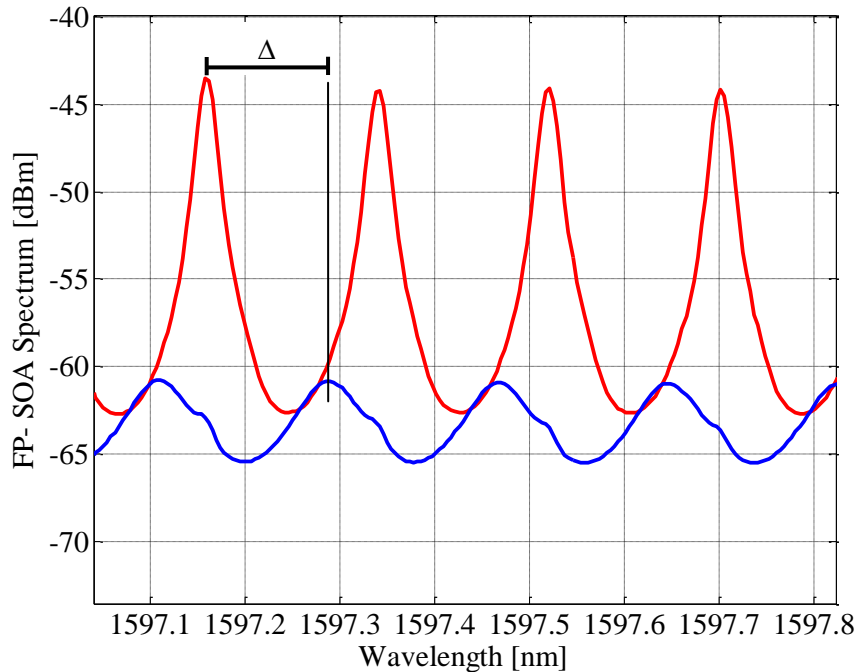


Figure 2.9: $\Delta = 0.68$ [-] between TE and TM modes

Moreover, this experimental investigation shows a variety of Δ values due to the different refractive indexes between the TE and TM of the FPSOA. The refractive index is different between the polarization modes of the FPSOA related to several factors such as material aspects (how photons interact with TE and TM modes) and geometric aspects (different confinement factor between the TE and TM modes). The FPSOA birefringence makes the FPSOA TE and TM resonances be in phase or out of the phase over the span of the gain spectrum.

2.5 Resonance Shifts with Injected Current

The refractive index has a nonlinear dependence on the carrier density in the active region of an FPSOA [15, 16]. The interference pattern will shift to the short or long wavelengths when the refractive index is changed. Furthermore, the gain of the

FPSOA resonances also depends on the carrier density in the active region. Figure 2.10 illustrates the gain and refractive index dependence on carrier density.

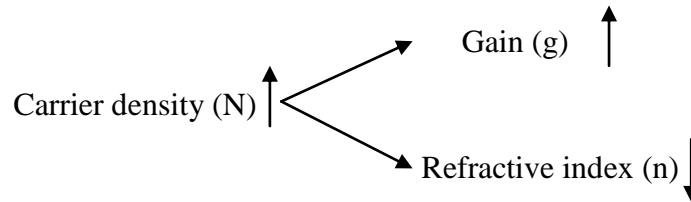


Figure 2.10: Gain and refractive index dependence on the carrier density.

When the carrier density increases in the active region of the FPSOA, the gain will increase and boost the peak power of the FP resonances. In addition, the refractive index will reduce. Reducing a refractive index will shift the FP resonances to the short wavelengths. On the other direction, if the carrier density reduces, this will reduce the optical gain and increase the refractive index simultaneously. Increasing the refractive index will shift FP resonances to the long wavelengths.

Figure 2.11 shows when increasing an external drive current into the FPSOA active region, the carrier density increases. This increment in the carrier density will increase the peak power of the standing waves and shift these standing waves to the shortest wavelength.

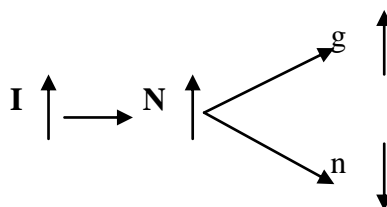


Figure 2.11: The carrier density dependence on the drive current value.

Figure 2.12 shows experimental results of increasing the drive current from 62 mA to 67 mA at temperature value of 20 C°. Figure 2.12 shows the dependence of a carrier density on an injected driving current. By tracking a one FP resonance as in Figure 2.12 (b); the peak power of this FP resonance increased by a 6.27 dB due to material gain increasing, and the refractive index reduced that shifted the resonant mode central wavelengths to the short wavelengths by an amount of 0.118 nm.

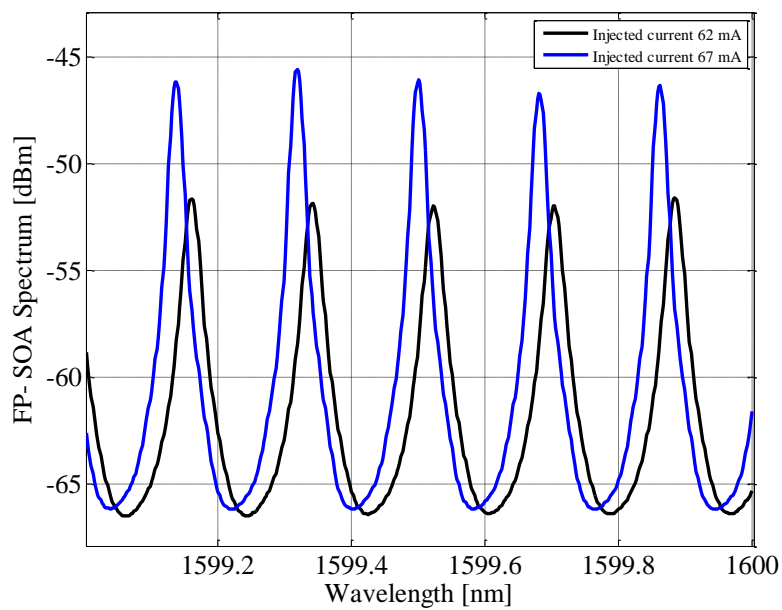


Figure 2.12: Resonant modes shift with injected current

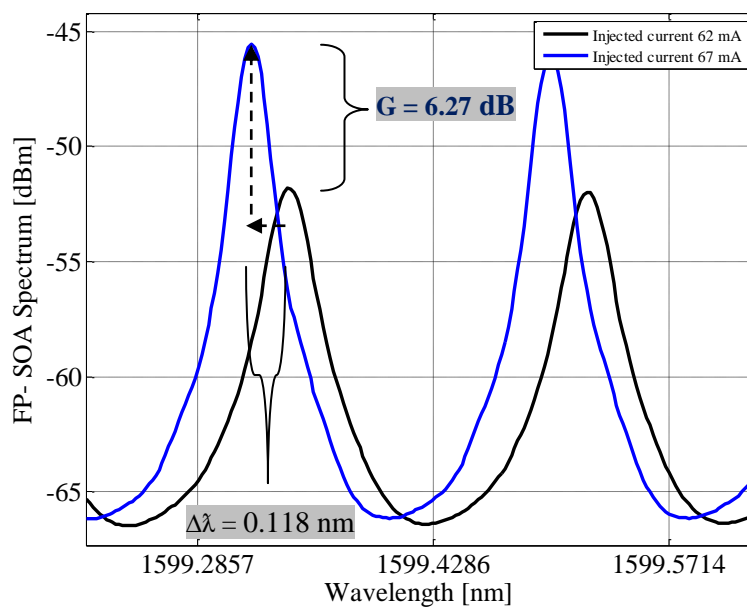


Figure 2.12: Zoom in FP resonances modes

The linewidth enhancement factor α characterizes the ratio of the refractive index change to the gain change when a carrier density is varied. In other words, this parameter describes the amount of shift in resonances. The amount of gain increment or decrement with the driving current alerts the carrier density in the active region of an FPSOA.

2.6 Resonance Shift with Input power

When optical signals are injected into the FPSOA, these signals deplete the carrier density in the active region [15]. This reduction in the carrier density will increase the refractive index value and reduce the optical gain inside the active region [15, 16]. In this process, the resonances of the FPSOA will shift to the long wavelengths as in Figure 2.13.

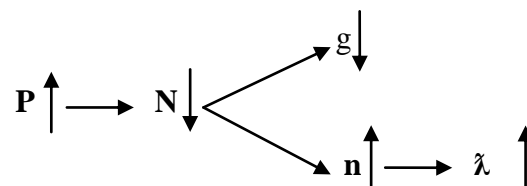


Figure 2.13: Dependence of the gain and the refractive index on input power

Figure 2.14 shows the experimental set-up schematic to examine the impact of different input optical powers into the FPSOA. The Mach-Zehnder Modulator (MZM) from EoSpace (model AX-0k5-12-PFA-S) is biased at the quadrature point. The optical CW signal generated from the Tunable Laser from Santec (model TSL-510). The TSL set values were gradually increased from -1 to 9 dBm. The central wavelength of these optical signals is 1590.8 nm. The Polarimeter (POD-101D) was used to measure the SOP of optical signals. The OSA was used to capture the output power from the FPSOA. The drive current from the LC was set to 62 mA at 20 C⁰.

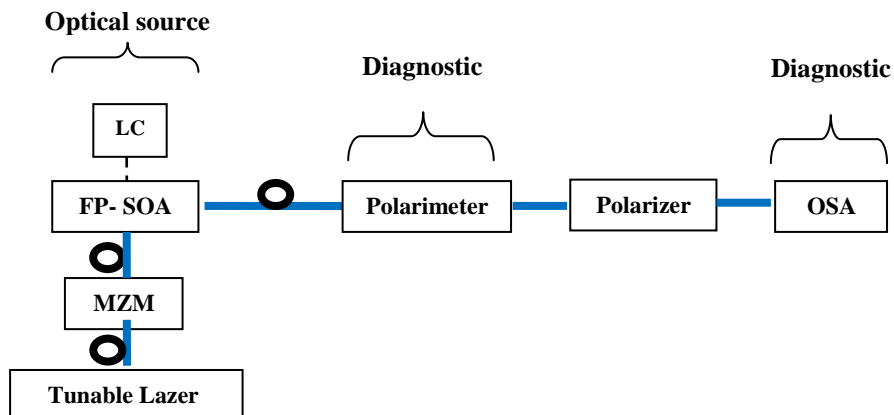


Figure 2.14: Experimental set-up of characterizing the impact of input optical signals on the FPSOA resonances

The PC before the MZM was used to align the input SOP to optimize the MZM output power. The four PCs before the FPSOA were used to force the total input power to experiences a TE mode. The four PCs after the FPSOA were used to align the TE mode of the FPSOA resonances to pass through the polarizer. The OSA was used to capture the impact of changing input power on the TE mode of the FPSOA resonances.

Figure 2.15 shows the wavelength shift and resonance peak power by tracking one resonance of the TE mode corresponding to each input power value. Input power values were varied from -1 to 9 dBm in the TSL. Increasing the input power depleted the carrier density that lead to increasing the refractive index and decreasing the gain. This figure shows the wavelength (λ nm) in y-axis where the resonance shift is increased when the refractive index increased. Moreover, this figure shows the resonance peak power decreasing when the gain is decreased as expected.

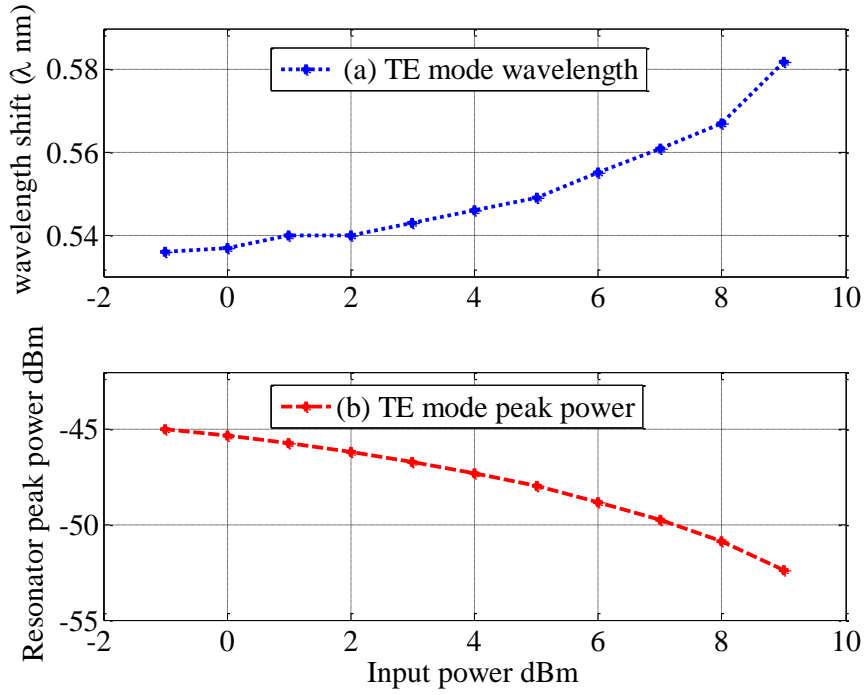


Figure 2.15: (a) A resonance wavelength shift associated with input power change
 (b) A resonance peak power involving with changing the input power value

2.7 Resonance Shift with Input SOP

Investigating the optical AND gate with polarization rotation requires characterizing the polarization modes of the FPSOA shift when launching the input signal power in both modes of the FPSOA. Each SOP value is representative by a ρ value. The ρ value quantifies the amount of total input power that propagates into the P^{TE} and P^{TM} of an input signal. Equations 2.2 and 2.4 show the amount of total input power (P_{in}) that decomposes into two orthogonal SOPs (P^{TE} and P^{TM}) according to ρ :

$$P^{\text{TE}} = \rho * P_{\text{in}}, \quad 2.2$$

$$P^{\text{TM}} = (1 - \rho) * P_{\text{in}}. \quad 2.3$$

The mathematical formula of ρ is obtained from the Stokes parameters as given below:

$$S_1 = P^{TE} - P^{TM}, \quad 2.4$$

$$S_1 = \rho P_{in} - (1 - \rho) P_{in}, \quad 2.5$$

$$S_1 = P_{in} [\rho - (1 - \rho)], \quad 2.6$$

$$\rho = \frac{1}{2} \left(\frac{S_1}{P_{in}} + 1 \right), \quad 2.7$$

$$P_{in} = P^{TE} + P^{TM} \approx P^{TE} + P^{TM} + P_{unpolarized}, \quad 2.8$$

$$P_{polarized} = \sqrt{S_1^2 + S_2^2 + S_3^2}, \quad 2.9$$

$$P_{in} = \sqrt{S_1^2 + S_2^2 + S_3^2} = S_0 \text{ DOP} \quad 2.10$$

$$\rho = \frac{1}{2} \left[\frac{S_1}{\sqrt{S_1^2 + S_2^2 + S_3^2}} + 1 \right] = \left[\frac{S_1}{S_0 \text{ DOP}} + 1 \right], \quad 2.11$$

$$\rho = 0.5 \left[\frac{\delta_1}{\text{DOP}} + 1 \right], \quad 2.12$$

$$\rho[-] = 0.5 [s_1 + 1]. \quad 2.13$$

When ρ equals one the total input power is injected into the TE mode of the FPSOA. Moreover, when ρ equals zero, the total input power is injected into the TM mode of the FPSOA.

Recalling Figure 2.14, the total input power set to 9 dBm at 1591 nm in the tunable laser. The ρ value was changed gradually from 0 to 1 [-] by a factor of 0.2. Figure 2.16 shows that the TE and TM modes of the FPSOA shift with each ρ set value. The y-axis tracks the central wavelength of one TE and TM resonance when changing the value of the ρ while the x-axis shows the ρ values from 0 to 1 [-].

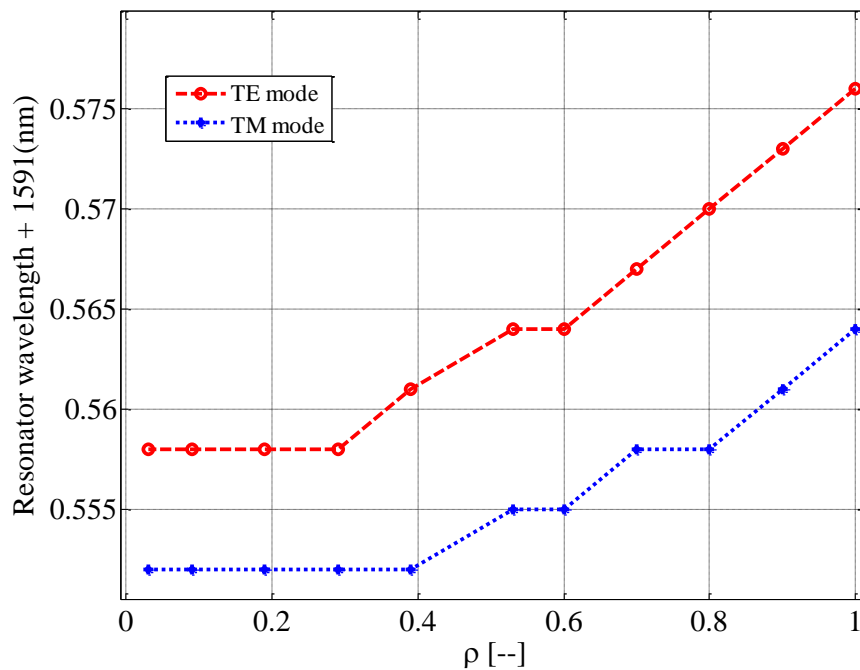


Figure 2.16: Characterizing ρ value impact on the TE and TM modes shift for fixed value of total input power into the FPSOA

This figure shows that the TE resonance wavelength has a value of 0.558 nm when ρ is zero, and this resonance shifts to the long wavelength value of 0.576 nm when ρ is one. In additional, this figure shows that the TM resonance wavelength has a value of 0.552 nm when ρ is zero, and this resonance shifts to the longer wavelength value of 0.564 nm when ρ is one.

In summary, this data shows for a fixed amount of total input power a longer wavelength shift when the total input power is optimized to propagate into the TE mode of the FPSOA ($\rho = 1$). Furthermore, this shows a short resonance shift for the same amount of the total input power when total input power is optimized to propagate into the TM mode of the FPSOA ($\rho = 0$).

The reason of having a longer wavelength shift when gradually increased ρ value toward ($\rho = 1$) is because the FPSOA is asymmetric in gain; asymmetric means the FPSOA provides a higher gain for the TE mode than the TM mode. When the ρ value equals one, a large amount of input power is injected into the TE mode of the FPSOA due to the waveguide geometry. Thus, this total input power depletes the carrier density value that increases the refractive index value. Increasing the refractive index value shifts the FPSOA resonances toward the long wavelengths.

When ρ value reduces from one, the internal power inside the FPSOA is reduced because a lower input power propagates into the TE mode of the FPSOA. Furthermore, the TM mode has a lower gain profile in the FPSOA due to the waveguide geometry. When the internal power reduces, the carrier density increases to compensate the lower power injected into the TE mode. Increasing the carrier density will reduce the refractive index and shift the resonant modes toward the short wavelengths as in Figure 2.16.

Furthermore, Figure 2.17 shows the TE and TM resonance peak power in the y-axis corresponding to the ρ value in the x-axis. This figure shows that a TE and TM resonances peak power is increased when the ρ value reduces from one to zero because the carrier density increased in the active region to compensate the low power injected in TE mode of the FPSOA. This Figure shows that a TE resonance has a peak

power of -49.12 dBm for $\rho = 1$, and this peak power increases to -46.66 dBm for $\rho = 0$.

The TE mode resonance experienced a gain of 2.46 dB.

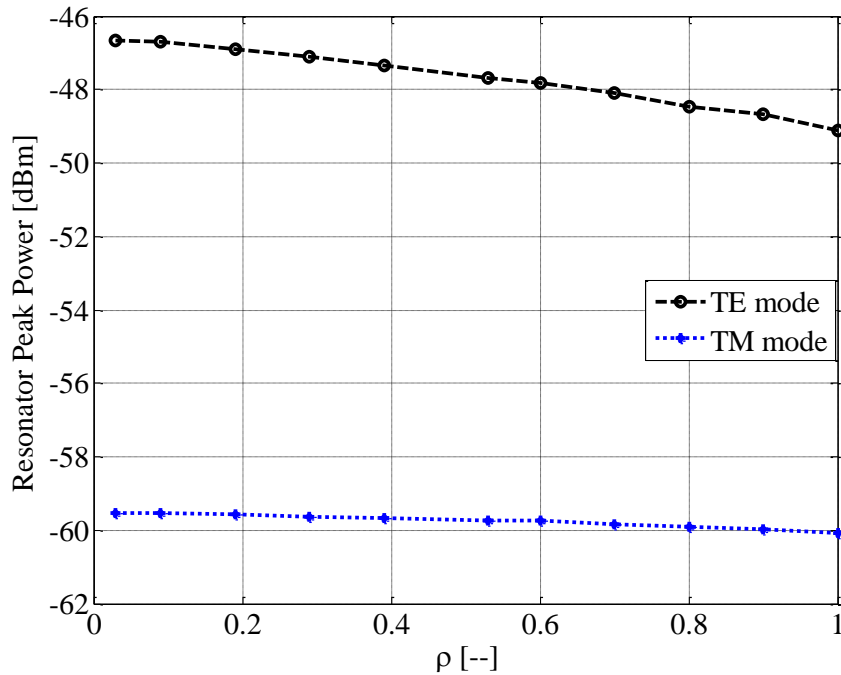


Figure 2.17: Characterizing ρ value impact on the TE and TM resonance peak power

In addition, a TM resonance has a peak power of -60.08 dBm for $\rho = 1$, and this peak power increases to experiences a -59.45 dBm for $\rho = 0$. The TM mode resonance experiences gain of 0.54 dB. In addition, this experimental result shows that the FPSOA is a polarization sensitive device. The polarization sensitivity means that the output of the FPSOA depends of the input SOP of an optical signal.

2.8 Optimizing Input Signal to Experience TE Mode

The optical signals of an optical AND gate require aligning their input SOP into the FPSOA due to the polarization sensitivity of this device. The basic operation an optical AND gate is established by aligning its optical signals to the TE mode.

Figure 2.18 shows a basic geometry of an FPSOA.

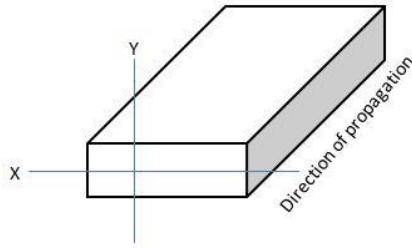


Figure 2.18: An FPSOA geometry axis.

Aligning the TE mode in parallel to x-axis plane of the FPSOA requires rotation of the polarization of the optical input signal, and forces it to experience the TE mode. In this case, the input power in P^{TE} is optimized to experiences the total amount of the input signal. In addition, the ρ value equals one, and the input power in P^{TM} is minimized.

The experimental procedures to optimize the total input power to experiences a TE mode is given:

- Recalling Experimental set-up 2.14, the first step is working with the FPSOA resonances without the optical signal power into the FPSOA.
- Recalling the procedures of obtaining TE and TM modes of the FPSOA in Section 2.3, the second step is getting the TM mode of the FPSOA resonances in the OSA trace.
- The OSA settings are a) resolution to 0.02 nm, b) set the OSA wavelength span function to two nm around the central wavelength of the input signal and, then c) set the OSA sweep function on repeat mode.
- After obtaining the TM mode of the FPSOA in the OSA trace, turn on the input power into the FPSOA.
- The third step is working on changing the PCs before the FPSOA while monitoring the peak power of the input signal in the OSA trace. The role of

these PCs is to minimize the peak power of the input power (P^{TM}) shown with the TM resonances. In other words, the process of changing these PCs is to rotate the polarization of the input signal and force the total input power to only propagate in the P^{TE} polarization component as shown in Figure 2.19.

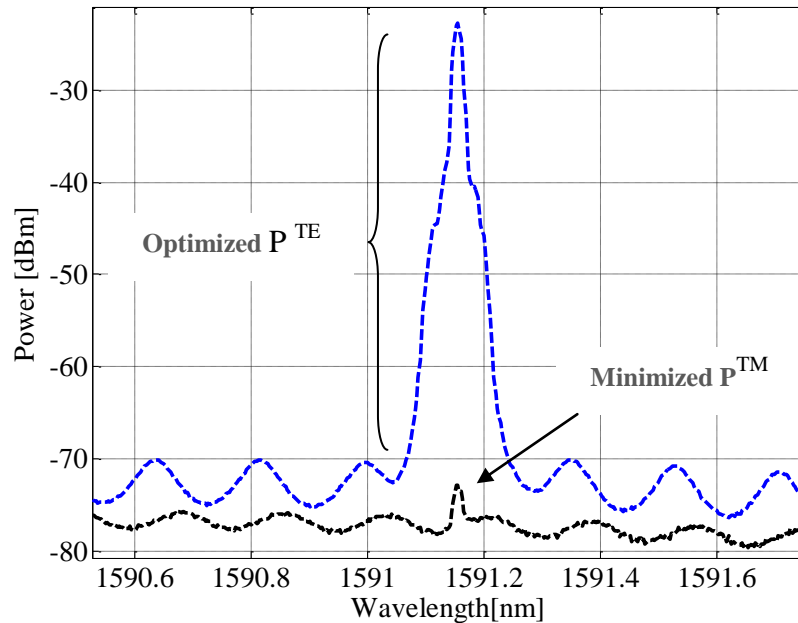


Figure 2.19: Optimizing input SOP to experiences a TE mode

Figure 2.19 shows the experimental result after optimizing the total input power to experiences a TE mode. This total input power is injected into the TE mode of the FPSOA cavity resonance. This figure shows a high peak power when the input power interacts with the TE mode of the FPSOA. Furthermore, this figure shows that the input power in the P^{TM} polarization component is minimized (little input optical signals propagate and interact with the TM mode of the FPSOA).

This chapter introduces important experimental steps that help to conduct the all optical AND gate in the following chapters. This chapter shows that the FPSOA output depends on the input signal conditions like power and SOP. Furthermore, this chapter provided an important understanding of input power impact on the FPSOA resonances shift.

Chapter 3

All-Optical AND Gate Based on the TE Mode

3.1 Introduction

In this chapter, an all-optical AND gate is demonstrated based on a Fabry-Pérot (FPSOA) cavity resonance and its strong nonlinearity. This chapter explains the basic concept of realizing an optical AND gate based on a resonance shift. Because an FPSOA is a polarization sensitive device, this chapter examines the AND gate contrast based on a specific state of polarization (TE mode) into the FPSOA. Furthermore, this chapter explains how to optimize the cross gain modulation (XGM), cross gain modulation (XPM), and cross polarization modulation (XPoIM) based on selective optical signal conditions such as input power, polarization state, and wavelength.

3.1.1 Principle of Operation

Recalling table 1.2 in Chapter 1 that illustrates the truth table of an optical AND gate, it has two input pulse signals (input A and input B). The main goal of this thesis is to enhance the contrast of output AB as compared with the other cases as shown in Figure 3.1. For the solitary input A pulse ($A= 1, B= 0$) case, or the solitary input B pulse signal ($A= 0, B= 1$) case injected into the FPSOA, the output AB should have an extremely low power. Figure 3.1 illustrates the basic operation of an optical

AND gate experiment. This figure shows the optical AND gate four different output AB cases.

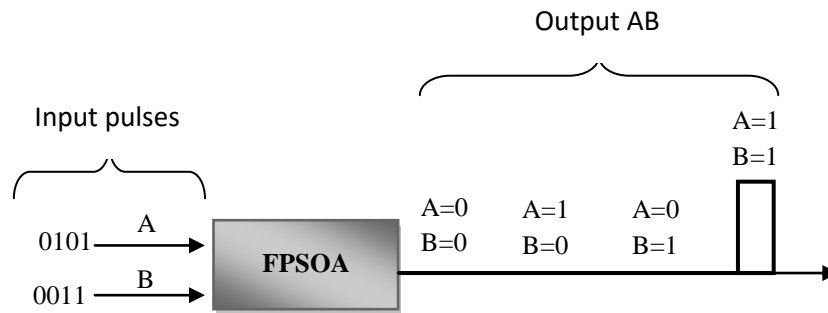


Figure 3.1: AND gate operation cases.

The basic operation of an optical AND gate is based on the digital transfer function of a FPSOA cavity resonance. The digital transfer function emerges from the nonlinear interaction between an optical input pulses and a cavity resonance in the active region of an FPSOA.

Figure 3.2 illustrates a digital transfer function for an optical AND gate. This digital transfer function relies on the nonlinear refractive index dependence on the carrier density in the active region of an FPSOA.

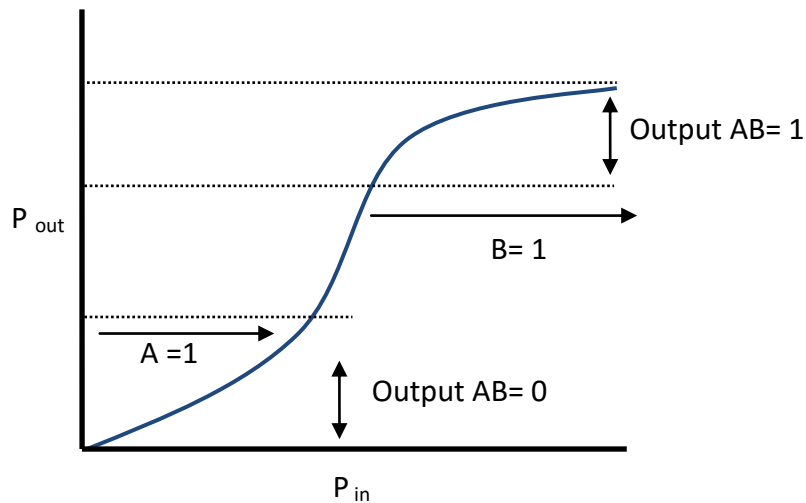


Figure 3.2: Digital transfer function of an optical AND gate.

When an input A pulse signal ($A = 1$) is injected into the FPSOA, this optical signal depletes the carrier density by simulated emission. Reducing the carrier density increases the refractive index. Increasing the refractive index shifts resonance modes toward the long wavelengths. However, this shift is not enough to place a FP resonance on top of input A pulse signal. Thus, the output AB for the $A = 1, B = 0$ case is in the transition stage of the digital transfer function. In addition, the gain of a FP resonance is not utilized yet.

When input B pulse signal ($B = 1$) is injected with an input A pulse signal ($A = 1, B = 1$), the shifting of a resonance is sufficient to place a FP resonance on top of input A pulse signal. When a FP resonant mode is placed on top of the input A signal, the input A pulse signal experiences resonance peak power gain, and the output AB experiences a high power (output $AB = 1$) as shown in Figure 3.2. It is important to control the input A and input B powers level and wavelength to optimize the digital function of the FPSOA.

3.1.2 Optical AND Gate and FPSOA Nonlinearities

Recalling Section 2.6, this Section explained the impact of an input power into the FPSOA resonant cavity. Changing the carrier density in the active region of an FPSOA induces strong nonlinearities. These nonlinearities depend on the nonlinear refractive index and material gain dependence on the carrier density of an FPSOA, and an input A pulse and input B pulse signal conditions (power, wavelength, and SOP) into the FPSOA cavity resonance. These nonlinearities have a great role for the investigating of the optical AND gate experiment in this thesis. This thesis studies several important nonlinear effects via nonlinear interaction between an input A pulse signal and input B pulse signal.

The general concept of these nonlinear phenomena is explained in Section 1.4.3 in Chapter 1. Cross phase modulation (XPM), cross gain modulation (XGM), and cross polarization modulation mode (XPolM) is investigated under different conditions of injected optical signal. Figure 3.3 explains the relationship between the carrier density (N), material gain (g), refractive index (n), and nonlinearities in an FPCOA.

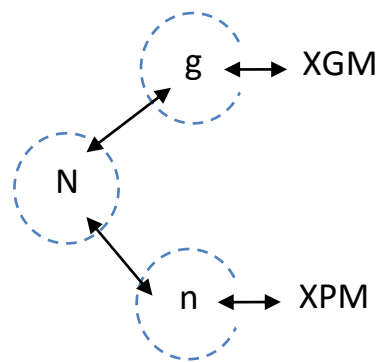


Figure 3.3: Nonlinearity dependence on carrier density.

Figure 3.3 illustrates the physical cause of nonlinear behavior in the FPCOA. When carrier density decreases due to an input power injected into the FPCOA, it reduces the material gain that reduces the peak power of the resonant modes. At the same time, the refractive index increases to shift the FP resonances toward the longer wavelength. The process of shifting exhibits nonlinear phenomena. The first nonlinear phenomenon is XGM, which changes the optical gain of one optical signal (A) due to another optical signal (B). The second nonlinear phenomenon is XPM that changes the phase of one signal (A) due to another optical signal (B). Furthermore, XPolM can happen where the polarization of one signal (A) is changed due to another signal (B).

3.2 Experimental Set up

The optical AND gate experimental set-up is illustrated in Figure 3.4. A continuous wave (CW) beam was generated from a Santec tunable laser (TSL-510V) for the input A optical signals. Input A wavelength is set to 1604.0420 nm with a -1.49 dBm power. A CW optical signal was generated from a Santec Tunable laser (TSL-210V) for the input B optical signals. The input B wavelength was set to 1599.3960 nm with a -4.25 dBm peak power.

A pulse generator (PG) pattern from Picoseconds Pulse Lab was used to feed the two Mach-Zehnder Modulators (MZMs) from EoSpace (model PM-OK5_10-PFA-PFA-S) with pulse of 10 ns pulse width. The MZMs were used to modulate the continuous waves of input A and B signals. The input A pulse signals pattern are (0101), and input B pulse signals pattern are (0011) with a return-to-zero (RZ) data format.

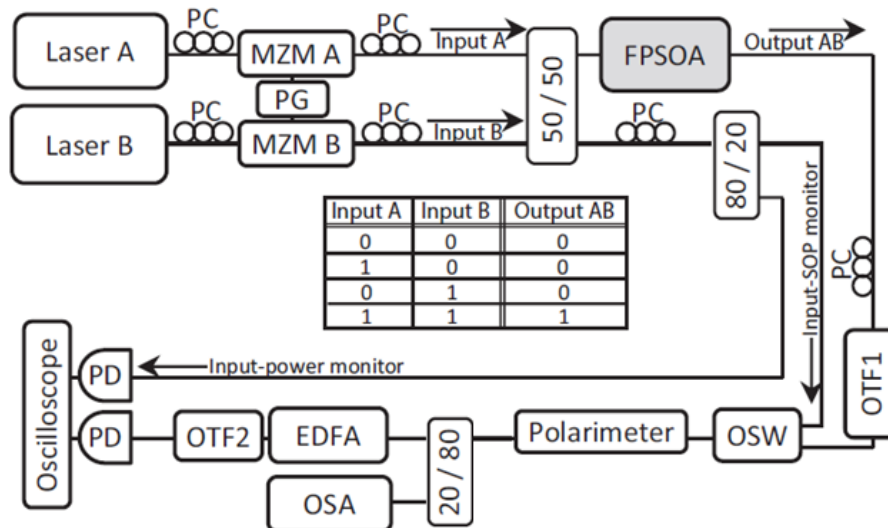


Figure 3.4: Optical AND gate experimental setup & truth table.

Both of these signals injected into the multi quantum well FPSOA. The laser controller (model LDC-3908) provides the external drive current (charge carriers) into the FPSOA active region. The laser controller set to provides 67 mA driving current (2.9 mA above lasing threshold) at a temperature of 20°. PCs are responsible for changing the orientation of light waves according to the propagation path. These PCs are classified in four categories according to their function in this experiment.

The first category is a PC before the MZM to change the polarization of the CW signals from the laser source to match the TE mode of the planer waveguide of the MZM, required to obtain a maximum output power. The second category is PCs after two MZMs. These PCs were used to set the TE mode state of polarization (SOP) for input A and input B signals into the FPSOA.

The third category is a PC in the input signal monitoring path before the 80/20 coupler. This PC was used to force the value of the Stokes parameter (S1) in the polarimeter to become one in the input SOP monitoring path. This means placing the input A SOP onto the S1 axis of the polarimeter. This placing should be performed after optimizing the input A to experience the FPSOA TE mode. Making S1 equal one helped to measure the other SOPs when the input SOP is moved away from the TE mode in Chapter 4. The last category located after the FPSOA is to control the SOP and have an improvement role when introducing a polarizer in Chapter 5 to enhance the contrast of the optical AND gate.

The optical switch (OSW) was used to switch between the output AB path after the FPSOA and input SOP mintoring path into the polarimeter. Thus, the polarimter can measure the input A and the output AB SOP. The optical polarimeter (POD-101D) with a 100 kHz bandwidth was used to measure the degree of

polarization (DOP), Stokes parameters, and state of polarization (SOP) of optical signals.

A bandwidth variable optical tunable filter (OTF1) from Alnair labs (model BVF-200CL) was used to validate the SOPs. This filter was used to remove out the unwanted wide range spectrum of amplified spontaneous emission (ASE) due to spontaneous emission in FPSOA active region. Furthermore, the optical tunable filter-300 (OTF2) from Santec was used to eliminate the optical noise from the Erbium-doped fiber amplifier (EDFA).

The EDFA is an L band amplifier from Amonics (Model AEDFA-L-PA-25-FA), and was used to amplify the output AB of optical AND gate signals. The two laser pump of the EDFA were set to 200 mA. Another important diagnostic is the optical spectrum analyzer (OSA-AQ6370B). This device has the advantage of characterizing the output AB spectrum cases of the optical AND gate. The last diagnostic is digital phosphor oscilloscope (Tektronix DPO4104) that receives the electrical signals from two 23 GHz PIN photodetector (PD) to temporally characterize the input signal into the FPSOA, and the AB optical pulses out of the optical AND gate.

3.3 Optical AND Gate Input Signals

The multi quantum well FPSOA is a birefringent. Section 2.4 in Chapter 2 has the experimental results that characterize the two modes (TE and TM modes). These results showed that the FPSOA is a polarization sensitive device due to nonlinear refractive indexes dependence on the carrier density. Furthermore, these results showed that TE resonant mode experiences more gain than the TM resonant mode. In this chapter, the optical AND gate input pulse signals are optimized to experience a

TE mode. Obtaining the TE mode is achieved in the experimental procedures that explained in Section 2.8 of Chapter 2. Working with TE mode result in an optical AND gate without polarization rotation in the FPSOA.

After obtaining the TE mode for input A and input B pulse signals, the PC in the input SOP monitoring path was used to calibrate the input A SOP on the S1 axis of the polarimeter. Because both input A and input B pulse signals are injected to the polarimeter by using a 3 dB coupler, it is impossible to measure the input A SOP in the polarimeter for the case of (A= 1, B= 1). Input A and input B have a different powers and wavelengths values. Consequently, it is important to measure the input A SOP in the case when only input A is injected into the FPSOA (A= 1, B= 0) to validate the measurement of the polarimeter.

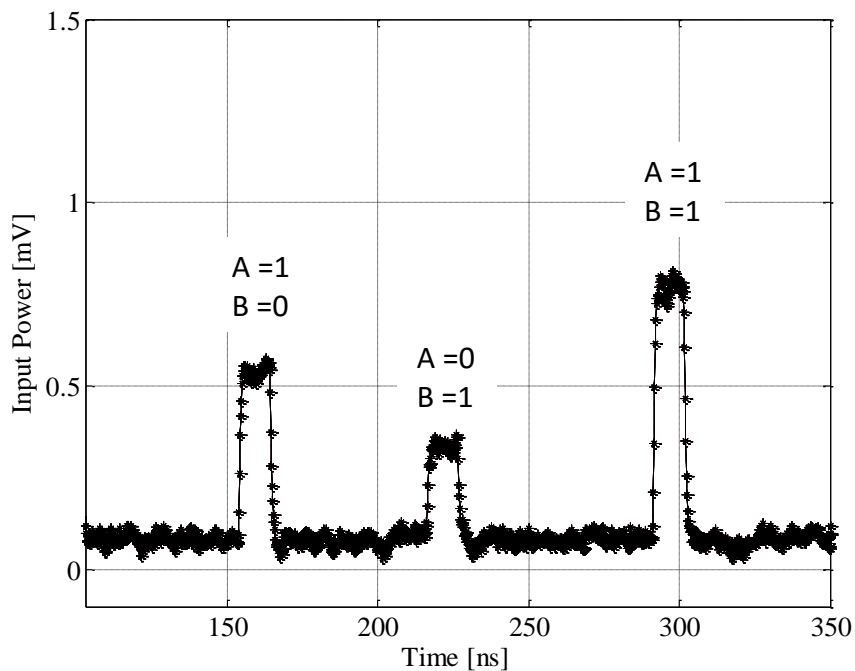


Figure 3.5: Optical AND gate input pulse signals.

Figure 3.5 characterize the four cases of optical AND gate input pulses signals before injecting them into the FPSOA. Input A pulse signals have a 10 ns pulse width and a peak power of -18.7 dBm including the coupling loss of 9 dB between the fiber

and FPSOA (fiber-to-SOA coupling loss); the input A pulse energy is 135 fJ. The input A wavelength is 1604.050 nm, which is longer than a FP resonance by 0.036 nm. These two values input power and wavelength were optimized during the experiment to obtain the highest contrast of the optical AND gate. The input A wavelength was chosen to work with wavelength difference $\Delta = 0.58$ [-] between the TE and TM modes. Defining the Δ is explained in Section 2.4 in Chapter 2. This Δ value means that the TM mode has a longer wavelength than the TE mode by 0.1044 nm.

The input B pulses have a 10 ns pulse width and a peak power of -22.2 dBm including the coupling loss of 9 dB between the fiber and FPSOA (fiber-to-SOA coupling loss); the input B pulse energy is 60 fJ. The input B wavelength is 1591.396 nm. This wavelength is chosen to overlap a TE resonance such that $\Delta = 0$ [-]. The input power and wavelength is optimized in this experiment to obtain the highest contrast AND-gate operation.

Cross phase modulation enables diversity between input A and input B wavelengths. Furthermore, this wavelength diversity enables the optical tunable filter (OTF 1) to remove the input B pulse signal after the FPSOA. Removing the B pulse signal after the FPSOA is important because the output AB data is associated with input A wavelength in this experiment. The output AB wavelength of optical AND gate is selected as input A wavelength. In addition, the polarimeter can correctly measure the SOP, DOP, and Stokes parameters of output AB signal.

3.4 Optical AND Gate Polarization

Table 3.1 shows the input SOP for the input A pulse signals for the case of A= 1 and B= 0. Because the polarimeter sampling rate is only 625-KSa/s, all SOP

measurements of input A pulses are obtained at continuous waves (CW) power to associate it with the OSA measurements; in this case, the PG is set to provide the maximum output power as CW peak power of input A pulses. Furthermore, this SOP is also measured when input A signal is modulated (data pattern) as a reference.

Input A	DOP	δ_1	δ_2	δ_3
CW pattern	96.4	0.9635	-0.0119	0.0228
Data pattern	84.1	0.8357	-0.0857	0.0286

Table 3.1: Input A with TE mode SOP into the FPSOA.

Table 3.1 shows the polarimeter measurements of DOP and Stokes parameters for the input A signal in the input SOP monitoring path after forcing the input A to have a value of $\delta_1=1$ (0.9635). Table 3.2 shows the normalized values by dividing the Stokes parameters with the DOP value, as discussed in Chapter 1.

Input A	DOP	s_1	s_2	s_3	ρ	Magnitude
CW pattern	96.4	0.99948	-0.01234	0.02365	0.9997	0.9998
Data pattern	84.1	0.99370	-0.10190	0.03401	0.9968	0.9995

Table 3.2: Normalized Stokes parameters of input SOP into FPSOA.

Equation 2.13 in chapter 2, this equation utilizes to get the ρ value for input A signal. For $\delta_1 = 0.9635$, $\rho = 0.9997$ for the input A signal with TE mode. In table 3.2, the magnitude of the Poincare vector represents the total polarized power of an input signal. If the Stokes parameters normalized, the magnitude should have value of one. Calculating the magnitude of the Poincare vector with normalized Stokes parameters is a check on this notion as discussed in Chapter 1. This value represents a point on the Poincare sphere surface of the unit sphere. Moreover, this point of the Poincare

sphere helps to know the SOP of the input A pulse required to experience a linear polarization for the TE mode.

3.5 Optical AND Gate Temporal Power

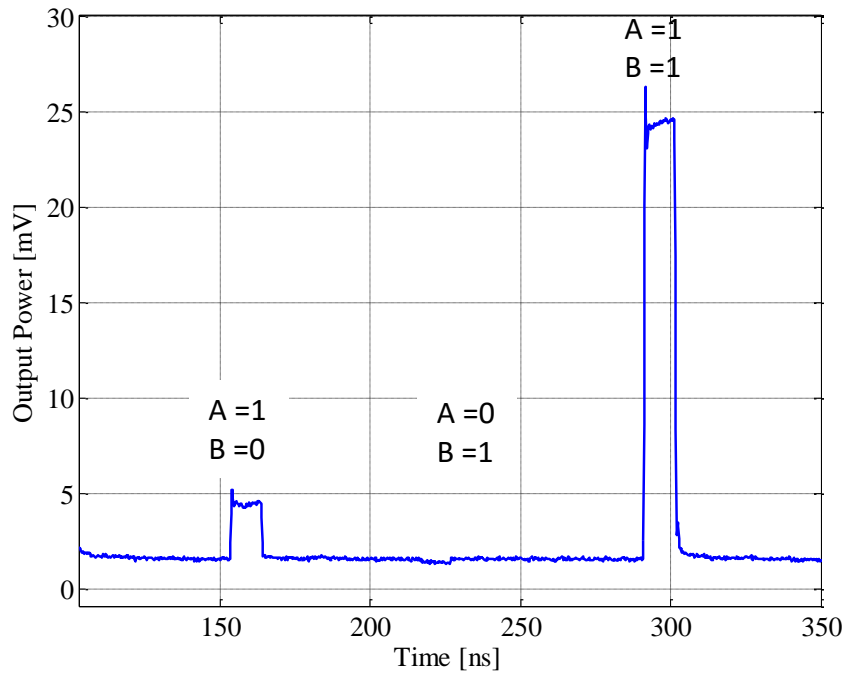


Figure 3.6 Output AB optical pulse signals of optical AND gate.

Figure 3.6 shows the output pulse signals from optical AND gate. The output AB of optical AND gate is shown for the four cases of input A and B pulses. When the input pulses set to represent (A= 0, B= 0) case and input (A= 0, B= 1) case, the output AB of this experiment showed an ideal operation and expected very low power. This proved that the OTF1 successfully stripped the B pulse after the FPSOA to support the functionality of the optical AND gate. Furthermore, when the input pulses set to represent (A= 1, B= 0), the output showed a low power signals of 4.45 mV.

The output AB exhibits a high output power when input A pulse signal and input B pulse signal are injected into the FPSOA (A=1, B=1). This case has a higher

power than the solitary the input A pulse signal ($A=1$ and $B=0$) case. The output AB has a 24.34 mV in the 23-GHz discovery semiconductor photodiodes (PD) for ($A=1$, $B=1$) case. The power increase occurs because introducing the input B signal saturates the gain in the active region of the FPSOA. Gain saturation reduces the carrier density that increases the refractive index. Increasing the refractive index shifts a FP resonance toward the input A pulse wavelength. Because an FP resonance shifts on top of the input A pulse signal, the input A pulse signal experiences high gain.

The contrast of the optical AND gate is detailed in Figure 3.7. Contrast $10 = 8.5$ dB. This contrast measured between the output AB power for the case of a dual input pulses ($A=1$, $B=1$) and the case of solitary input A pulse ($A=1$, $B=0$). The other contrast value (Contrast 01 and Contrast 00) are larger and therefore do not limit the AND gate performance.

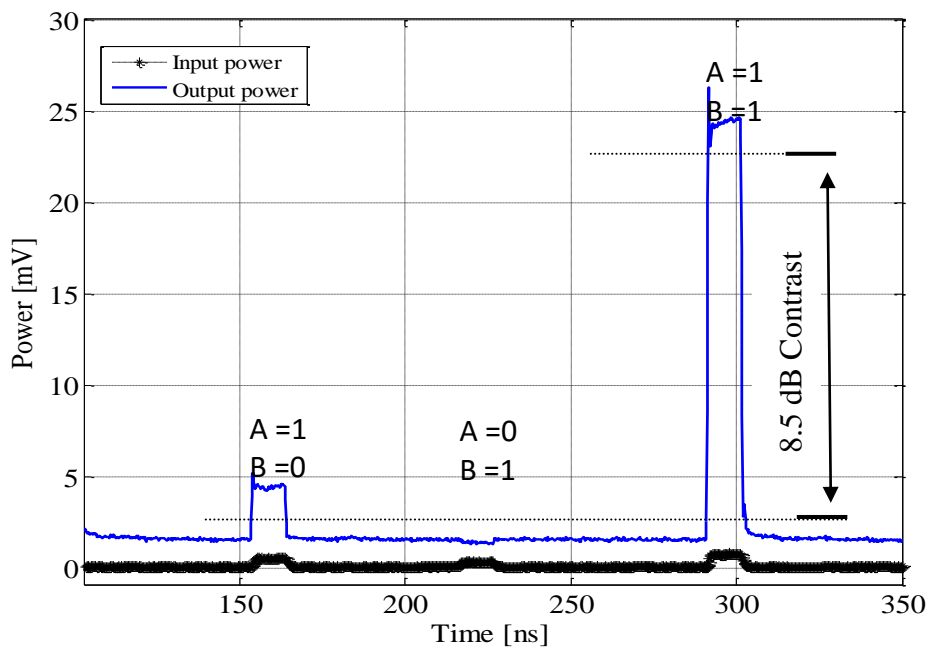


Figure 3.7 Optical AND gate output AB contrast.

Contrast₁₀ is the limiting AND gate contrast operating with TE mode. It is less than but near theoretical limit of 10 dB [3]. This investigation shows that even if

an input A pulse and input B pulse experience a TE mode that has a high gain, the output AB contrast is limited. Similar performance was shown by previously research [3-4]. Chapter 5 investigates a new technique that has used before to improve the contrast in optical flip-flop experiment [5]. This technique improves the contrast of our research by over 24 dB.

3.6 Optical AND Gate Spectral Power

Figure 3.8 shows the output spectrum of the input A optical as a CW to avoid low averaged values in the OSA. This figure shows that tuning the wavelength input A to the closest FP resonance is necessary to obtain the highest peak power via XPM when introducing input B signal that shifts the closest FP resonance on top of input A signal. The wavelength of the input A signal has been optimized to give the largest Contrast 10.

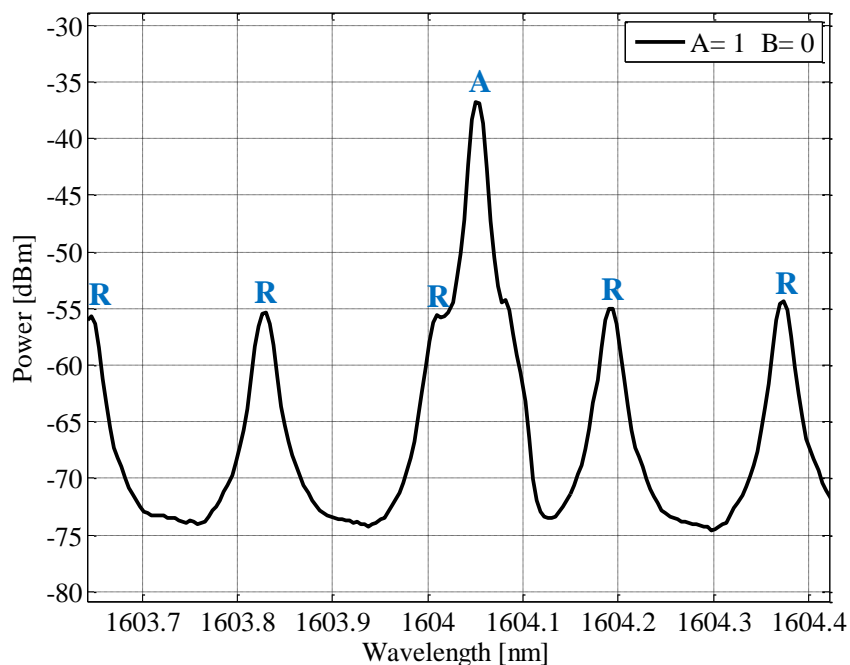


Figure 3.8: Output A signal optimized spectrum. R denotes a FPSOA resonance and A denotes the input A Signal.

Figure 3.9 shows the spectral contrast of the optical AND gate. The contrast is 8.5 dB between the output AB power between the case of a dual input pulses ($A=1$, $B=1$) and the case of solitary input A pulse ($A=1$, $B=0$). When input B is introduced into the FPSOA with the input A signals, the resonances shift to the right side toward the input A wavelength via the XPM. The output AB power becomes high when the A signal experiences the resonance gain. For the case of $A=1$, $B=0$, the output AB has less power as shown in Figure 3.8. It is important to note that the contrast was measured to be the same whether using the oscilloscope or the OSA.

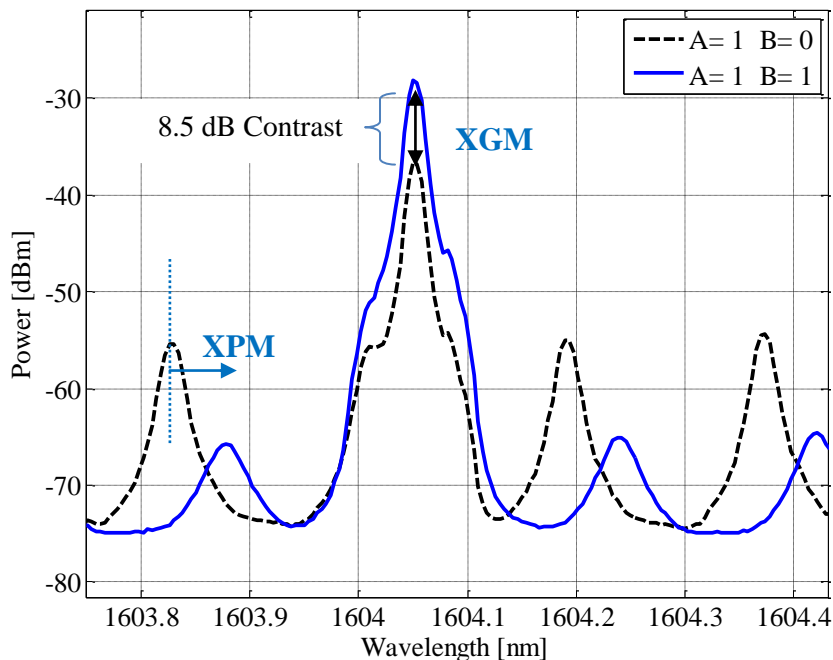


Figure 3.9: Output AB spectrum contrast of optical AND gate.

Figure 3.10 shows the optical AND gate spectrum for all cases ($A=0$, $B=0$), ($A=0$, $B=1$), ($A=1$, $B=0$), and ($A=1$, $B=1$). This figure shows the resonance wavelength shift involving when the carrier density depletes due to introducing the input A and input B signals into the FPSOA cavity resonance. The resonant modes shift from the short to long wavelengths due to the increasing of the refractive index. By tracking as a resonance, the shift between the $A=0$, $B=0$ case and $A=1$, $B=1$ case

is 0.052 nm. Moreover, this figure shows the peak power for each case of the optical AND gate. The resonances peak power drops because the internal material gain is reduced when the carrier density is depleted by optical AND gate injected signals. By tracking one resonance, the peak power drop between (A= 0, B=0) case and (A= 1, B= 1) case is 11.83 dB.

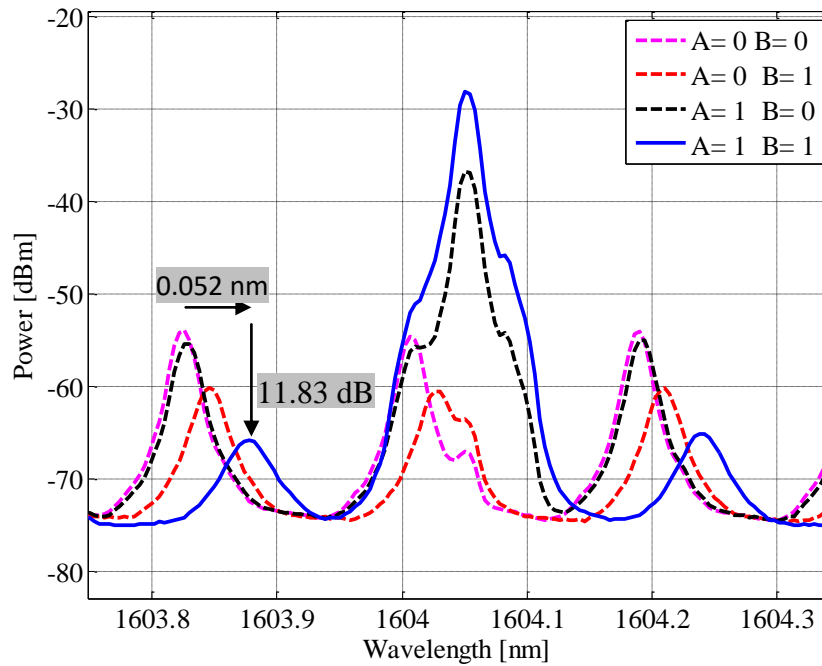


Figure 3.10: Optical AND gate spectrum under different signal conditions.

Chapter 4

Polarization Rotation during Optical AND Gate Operation

4.1 Introduction

This Chapter investigates optical AND gate operation that is accompanied by polarization rotation. To achieve polarization rotation, the input A pulse signal is injected into both polarization modes of the FPSOA. This chapter characterizes the output AB SOP on the Poincare sphere; the Poincare sphere is used as a guide to characterize polarization diversity.

4.1.1 Principle of Operation

Section 3.1 in Chapter 3 explained the basic operation of an optical AND gate, and discussed the basic concept of the digital transfer function of an optical AND gate. The basic action of the digital transfer function emerges from a nonlinear interaction between an input signal and a cavity resonance of an FPSOA. Whereas Chapter 3 investigated the optical AND gate using the TE mode for the input A SOP, this chapter aims to operate the optical AND gate by moving the input A SOP away from the TE mode. This means injecting the input A pulse in both polarization modes (TE and TM modes) of the FPSOA.

4.1.2 Optical AND Gate and Polarization Rotation

We use polarization rotation to optimize the output AB high power state of an optical AND gate when input A and input B enter an FPSOA together. At the same time, we minimize the output power when a solitary input A pulse or input B pulse enters an FPSOA. Polarization rotation is investigated under controlled input SOP, input power, and wavelength of both input signals.

The basic operation of an optical AND gate via the polarization rotation is achieved by launching the input A pulse into both TE and TM modes of the FPSOA. Input A pulse undergoes polarization rotation because an FPSOA is a polarization sensitive device. This polarization sensitivity is due to both birefringence and anisotropic gain. Birefringence means the refractive index has different values for the TE and TM modes. Anisotropic gain means that an FPSOA has polarization dependent gain; my FPSOA exhibits higher gain for TE mode than the TM mode. the FPSOA has anisotropic gain due to different confinement factor for each mode. In other words, anisotropic gain depends on geometry specifications of an FPSOA; such geometry specifications are width of the active region and thickness of the waveguide.

Furthermore, the FPSOA exhibits different nonlinear phenomena; such phenomena are cross polarization modulation (XPoM), cross gain modulation (XGM), and cross phase modulation (XPM). These nonlinear phenomena are explained in Section 3.1.2 in Chapter 3. For example, a resonant mode shifts due to XPM. Furthermore, the input A pulse experiences extra gain from a FP resonance gain when the FP resonance is placed on top of this pulse. XPoM can happen when launching an input A pulse into both TE and TM modes of the FPSOA and input A pulse experiences XPM and XGM simultaneously. XPoM is responsible for output AB SOP rotation. This rotation is measured via the Poincare sphere between solitary

input A case ($A = 1, B = 0$) and both input A and input B case ($A = 1, B = 1$) of an optical AND gate.

4.2 Experimental Setup

Recall Figure 3.4 in Chapter 3 that illustrates the experimental set-up of an optical AND gate via TE mode. That experimental approach is followed in this chapter. The difference in this chapter is to adjust the input A SOP away from the TE mode. Assigning a specific SOP for input A pulse signal is achieved by changing the polarization controllers (PCs) after MZM A in Figure 3.4.

The PCs role is to change the orientation of input A SOP to feed both TE and TM modes with part of the total input power. Thus, the total input power will split into both polarization modes of the FPSOA. The input A SOP is optimized in this experiment to achieve the highest polarization rotation for input A SOP. The ρ for the TE mode is corresponds to 1 in the monitoring path. Thus, this alignment helped to measure the amount of polarization rotation.

4.2.1 Optical AND gate via Polarization Rotation

Recall Figure 3.5, which shows the input profile of both the input A and input B optical pulses. The input B pulse signal conditions will remain the same as those of Chapter 3. The input B pulses have a 10 ns pulse width and a peak power of -22.1 dBm including the 9 dB fiber-to-SOA coupling loss. The input B wavelength remained the same as 1591.396 nm. The input B SOP continued to experience the TE mode. The input A pulse peak power is still -18.7 dBm including the 9 dB fiber-to-SOA coupling loss. The input signal profile is shown in Figure 3.5.

The input A wavelength was tuned to 1604.042 nm in case of polarization rotation. The reason for tuning the input A wavelength is to optimize the optical AND

contrast. The previous wavelength was set to 1604.05 nm when input A experienced the TE mode only. In this chapter, the input A wavelength is shifted toward the closest FP resonance by 0.008 nm to compensate for a lower power injected into the TE mode due to the new input A SOP alignment.

The reason behind this compensation was first discussed in Section 2.7 in Chapter 2. When input A SOP is rotated away from the TE mode, the total input power split into the TE mode and TM mode of the FPSOA. A input A SOP rotated by 54.1 degrees, corresponds to 34.4% and 65.6% of the total input power injected into the FPSOA TE and TM modes, respectively. Because an FPSOA has an asymmetric waveguide geometry, the FPSOA provides more gain for the TE mode than the TM mode. Thus, the total internal power inside the active region reduced when part of the total power propagated in TM mode.

When the total internal power is reduced, the carrier density increased. Consequently, when the carrier density increases, the refractive index reduced. Reducing the refractive index shifted the FP resonance towards the shortest wavelength. This explains the physical reason of tuning the input A wavelength by 0.008 nm to experience the same separation when input A SOP experienced TE mode alone.

Table 4.1 shows the input A SOP for solitary input A case ($A = 1, B = 0$). This SOP is measured by the calibrated polarimeter as a guide. This SOP is measured using the peak pulse power emulating continuous waves (CW). CW is preferred because the polarimeter bandwidth sampling rate is only 625-KSa/s. In addition, this SOP measured when input A signal is modulated (pulse signals) is given in the second row. This SOP corresponds with the scope input measurement.

Input A	DOP	δ_1	δ_2	δ_3
CW pattern	93.8	-0.2936	0.8864	-0.0918
Data pattern	73	-0.2734	0.6763	-0.036

Table 4.1: Input A SOP via polarization rotation into the FPSOA.

Table 4.1 shows a low value of DOP (73) for a data pattern measurement. Because a data pattern has high and low peak input power, this two different input peak power, the polarimeter measuring gain value was not consistent. Thus, it is important to measure the SOP when the input A set to experience only its peak power, resulting in a stable power into the polarimeter. Table 4.2 shows the normalized values by dividing the Stokes parameters by the DOP value:

Input A	DOP	s_1	s_2	s_3	ρ	Magnitude
CW pattern	93.8	-0.31301	0.94499	-0.09787	0.3435	1.0003
Data pattern	73	-0.37452	0.92644	-0.04932	0.3127	1.0005

Table 4.2: Normalized stokes parameters of input A SOP.

Recall Equation 2.13 in Chapter 2. This equation is used to get the ρ value for input A signal. After solving it for $s_1 = -0.31301$, $\rho = 0.34$ for input A signal away from TE mode. The ρ value indicates that 66 % of the total power is injected into the TM mode while 34 % of the total power is injected into the TE mode of the FPSOA.

As results of moving input A SOP from TE mode, the ρ value shows that the input A polarization rotated by 54 degrees from TE mode. The magnitude of the Stokes parameters is representing by total polarized power of an input signal. When the Stokes parameters are normalized, the magnitude is limited to unity value to

produce the Poincare sphere as explained in Section 1.5.3 of Chapter 1. Figure 4.1 represents the input SOP for the input A SOP that experiences TE mode (SOP1). In addition, this figure shows the input A SOP that experiences polarization rotation (SOP2).

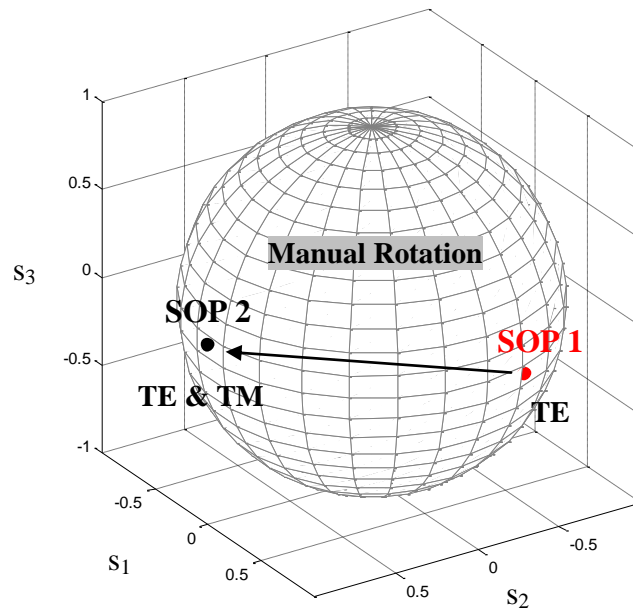


Figure 4.1: Input A SOP manual polarization rotation.

Figure 4.1 shows the input A SOP aligned to the TE mode that was investigated in Chapter 3 as SOP 1. Moreover, this figure shows the SOP 2 after rotating the polarization of input A pulse by 54 degrees. SOP 2 has a slight elliptical SOP pattern because it occurs between the equator and the pole of the Poincare sphere. This figure shows the polarization diversity of the input A SOP.

Figure 4.2 shows the output AB power profile of an optical AND gate undergoing polarization rotation. Based on oscilloscope trace, the contrast is 8.5 dB between the dual input A pulse signal and input B pulse signal case ($A=1, B=1$) and the solitary input A case ($A=1, B=0$). This figure shows that the output AB power is 19.4 mV for input case $A=1, B=1$, and the output AB is 4 mV for input case $A=1,$

$B=0$. The other two output AB for inputs $(A=0, B=0)$ and $(A=0, B=1)$ cases are extremely low and fell within the noise floor of the oscilloscope.

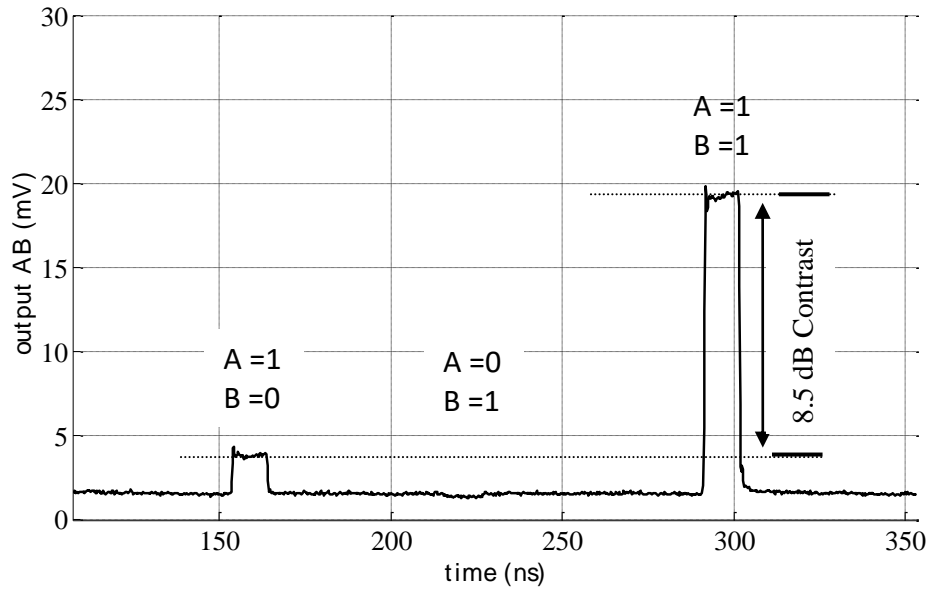


Figure 4.2: Optical AND gate output AB undergoing polarization rotation.

This figure shows the optical AND gate undergoing polarization rotation that can have the same contrast as input A SOP via TE mode in Chapter 3. Even though the experimental result via the oscilloscope trace showed a similar output AB profile in Chapter 3, this experimental result showed distinct input A SOPs in polarimeter measurement as shown in Figure 4.1. In other words, Chapter 4 helps to characterize the polarization sensitivity of the FPSOA to produce polarization diversity between optical AND gate input cases $(A=1, B=0)$ and $(A=1, B=1)$. Because of input polarization diversity, the output AB SOP should show polarization diversity because the FPSOA is a polarization dependent device.

Input A	DOP	δ_1	δ_2	δ_3
CW pattern	89.6	-0.4426	0.7674	0.1364
Data pattern	67.6	-0.1895	0.5766	-0.2984

Table 4.3: Output AB SOP for the input A=1, B=0 case.

The output SOPs are summarized in Table 4.3 for the input A= 1, B= 0 case. This Table shows the Stokes parameters for the output AB when solitary input A (A=1, B=0) into the FPSOA. Table 4.4 shows the normalized Stokes parameters to place on the surface of Poincare sphere.

Input A	DOP	s_1	s_2	s_3	ρ	Magnitude
CW pattern	98.9	-0.3361	0.5057	-0.7804	0.253	1.0004
Data pattern	82.4	-0.2714	0.5429	-0.5571	0.3598	1.0005

Table 4.4: Normalized output AB SOP for the input A=1, B=0 case.

The output SOPs illustrated in Table 4.5 for the input A=1, B=1 case:

Input A	DOP	δ_1	δ_2	δ_3
CW pattern	98.9	-0.3361	0.5057	-0.7804
Data pattern	82.4	-0.2714	0.5429	-0.5571

Table 4.5: Output AB SOP for the input A=1, B=1 case.

This table shows the Stokes parameters for output AB when both input A and input B (A= 1, B= 1) enter the FPSOA. Table 4.6 shows the normalized Stokes parameters.

Input A	DOP	s_1	s_2	s_3	ρ	Magnitude
CW pattern	98.9	-0.33984	0.51132	-0.78908	0.3301	0.9998
Data pattern	82.4	-0.32937	0.65886	-0.67609	0.3353	0.9998

Table 4.6: Normalized output AB SOP for the input A=1, B=1 case

Figure 4.6 shows the corresponding AB SOPs for the output AB on the Poincare sphere. These SOPs correspond to output AB SOPs for inputs A=1, B=0 and A=1, B=1 cases.

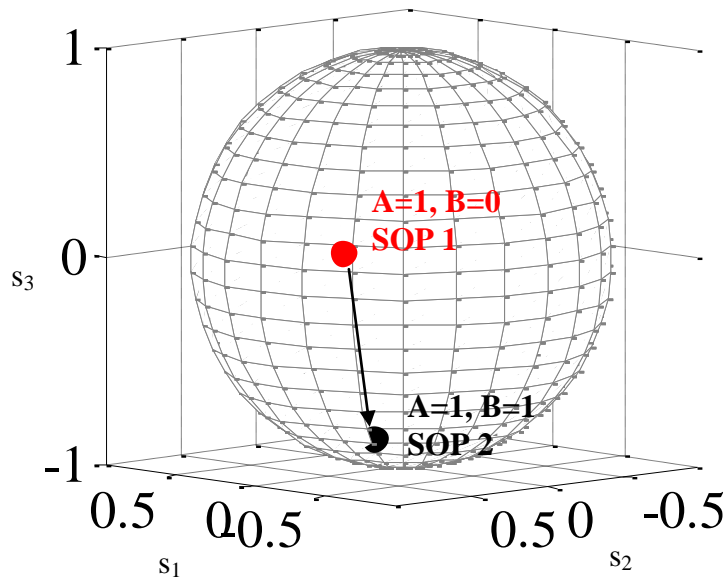


Figure 4.3: Output AB SOPs on the Poincare sphere.

This figure shows the polarization diversity of output AB SOPs, Each case exhibits a distinct SOP on the Poincare sphere. The output AB has distinct SOPs because the input A SOP undergoes polarization rotation that rotates the output AB from the SOP1 of input (A=1, B=0) case to the SOP2 of input (A=1, B=1) case. The two output AB SOPs are separated by 60.9 degrees on the sphere. This separation corresponds to $60.9/180$ equal to 33.9 % orthogonality.

Figure 4.4 shows the optical AND gate output AB operation accompanied by polarization rotation and the distinct SOPs along the oscilloscope trace for the output AB cases.

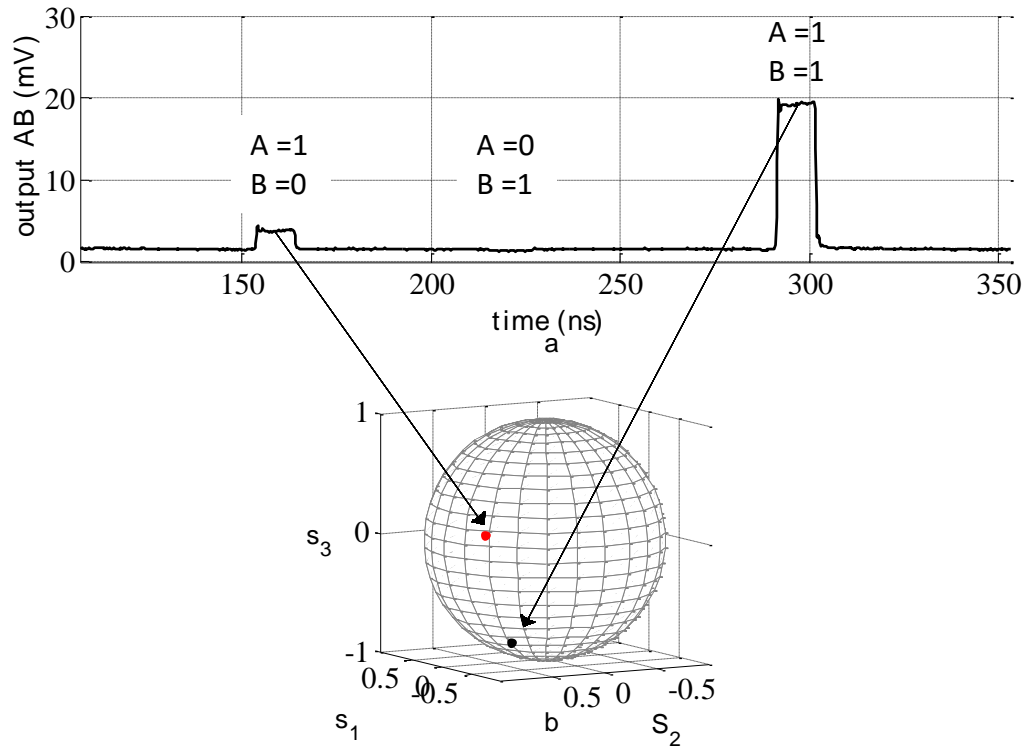


Figure 4.4 (a) Optical AND gate output AB profile accompanied by polarization rotation (b) Output AB SOPs corresponding to output AB oscilloscope trace.

When the input B injected into the FPSOA for the input case (A=1, B=1), three important nonlinearities occurred. The input B pulse depleted the carrier density in the active region of the FPSOA. Reducing the carrier density increases the refractive index, which shifts a FP resonance toward the input A pulse central wavelength via XPM. In addition, input A experienced higher resonance gain although the martial gain reduced via XGM.

Furthermore, XPolM occurs because of anisotropy in both the optical gain and refractive index of FPSOA. In addition, the FPSOA birefringence makes the TE and TM resonances be in phase or out of phase of spectral alignment over the span of the gain spectrum. Thus, the input A SOP experienced a polarization rotation that corresponding to rotate the output AB SOP due to the polarization sensitivity of the FPSOA.

The TM mode falls 0.1036 nm longer than the TE mode. The input A pulse central wavelength is 1604.042 nm; the closest FP resonance for TE mode wavelength is 1604.0136 nm (the location of this FP resonance before the input A wavelength). The closest FP resonance for the TM mode wavelength is 1603.91 nm (the location of this FP resonance after the input A wavelength).

Recall Equation 2.2 in Chapter 2 to find the normalized wavelength difference Δ [-], after solving the equation the $\Delta = 0.576$ [-]. This values means the TM mode does not have the same single-pass phase as the TE mode of the FPSOA. In this way, the gain and refractive index is different that leads to introduce a high value of polarization rotation.

Figure 4.5 explores the SOA spectrum traces using a CW signal patten for the optical AND gate input signals. A CW pattern is used to verify the OSA measurement. The OSA spectrum traces show the four output AB cases of the optical AND gate; these cases are corresponding to the input cases (A= 0, B= 0), (A= 0, B= 1), (A= 1, B= 0), and (A= 1, B= 1). When input case is (A= 0, B= 0), the FP resonant mode spectrum shows a high peak power. Furthermore, these resonances have a short wavelength value compared to the remaining cases. In this case, both input A and

input B are blocked from entering the FPSOA cavity. Thus, all the FPSOA gain is utilized to amplify the ASE.

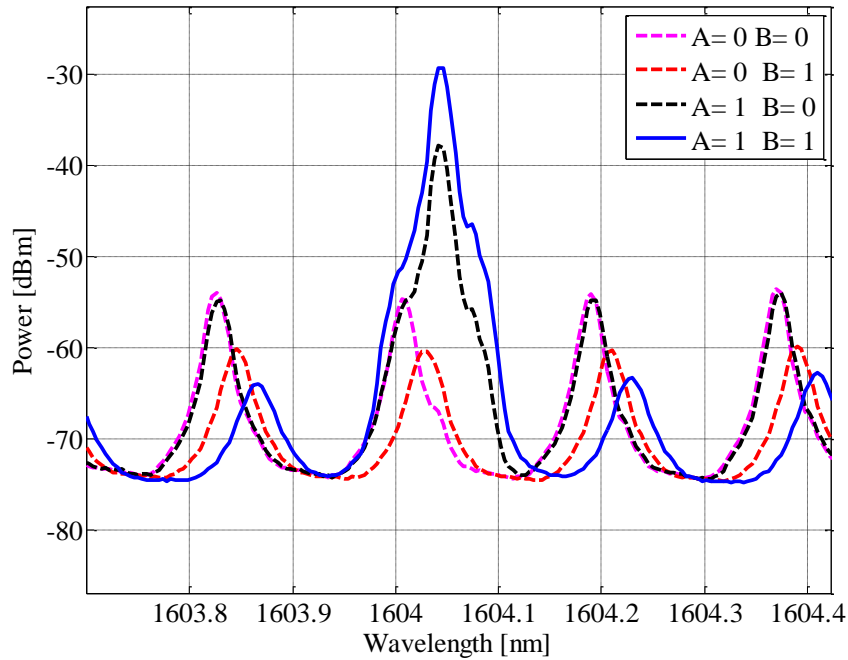


Figure 4.5 Optical AND gate SOA traces under different input conditions.

When the input case is $A=0, B=1$, the input B signal solely entered the FPSOA cavity. This signal depleted the carrier density in the active region. The material gain of the FPSOA is utilized to amplify the input B signal and resonant modes. This explains why resonant peak power dropped down due to gain when carrier density is reduced. In addition, reducing the carrier density increases the refractive index. Increasing the refractive index shifted resonant modes to the long wavelengths. Furthermore, when the input case is $A=0, B=1$, the input B SOP is set to experiences a TE mode ($\rho = 1$). This means the total input power in the TE mode of the FPSOA. Because the FPSOA has a higher gain for the TE mode, the input B experience the highest value of the material gain and shows a significant change due to carrier density, resonant mode peak power and shift.

When the input case is $A=1, B=0$, the resonant peak power has less dropped power than $A=0, B=1$ case. Moreover, the resonances shift is less even if the input A peak power (-18.6 dBm) that enters the FPSOA is higher than input B peak power (-22.1 dBm). This case showed less resonant shifting because input A SOP moved from the TE mode. When ρ moved from 1 to 0.3435 for this input case ($A=1, B=0$), this leads to an increase the carrier density because the total internal power is less in the TE mode direction. Thus, the resonances show high peak power and less wavelength shift compared to the input case ($A=0, B=1$).

When both signal A and B are injected together into the FPSOA, the carrier density reduces due to an increase the total internal power. This reduction increases the refractive index and shifts the FP resonances toward the input A signal wavelength. Furthermore, reducing the carrier density leads to reduce the material gain. Thus, the resonance peak power dropped down. The contrast is 8.5 dB between the dual input pulse signals ($A=1, B=1$), and the solitary input A ($A=1, B=0$) into the FPSOA.

Even if conducting the optical AND gate accompanied by polarization rotation showed a poor contrast, significant polarization diversity in output AB SOP has been demonstrated. Chapter 5 takes the advantage of the output AB polarization diversity in Chapter 4. Chapter 5 uses a new technique that controlling the output AB SOP after the FPSOA output to achieve a 31.2 optical AND gate contrast.

Chapter 5

Contrast Enhancement of

All Optical AND gate

5.1 Introduction

Investigating the optical AND gate in Chapter 3 and 4 demonstrated a 8.5 dB contrast. This finding showed a contrast limitation that is considered in-line with previously reported experimental data [3, 4]. Chapter 3 conducted an optical AND gate by aligning the state of polarization (SOP) of input signals with the TE mode. Chapter 4 conducted input A SOP to undergo polarization rotation.

The experimental result in Chapter 4 shows polarization diversity in output AB SOP between the dual input case ($A = 1, B = 1$) and solitary input A case ($A = 1, B = 0$). The output AB experienced polarization diversity because of polarization rotation. Polarization rotation is a key factor in this thesis and has not been investigated before to conduct an optical AND gate. In this chapter, a new technique is used to align the output AB SOP. This technique benefits from the polarization diversity in the output AB SOP.

Polarization rotation forces the output AB to produce a distinct SOP for the high-state power where this SOP is different from the low-state power SOP. A linear polarizer is used to block the low-state power SOP after aligning this SOP to the blocking axis of the polarizer. This technique helped to achieve a 31.2 dB of the

optical AND contrast that exceeded the previous demonstration data by over 24 dB (250:1) for such FPSOA device.

5.1.1 Principle of Operation

Recall Section 3.1 in Chapter 3. This section explained the operation principle of the optical AND gate based on the FPSOA cavity resonance. An optical AND gate benefits from a digital transfer function that emerges from a nonlinear interaction between an input signal and a FP resonance. Controlling the input A and input B signal condition such as input power, and wavelength, and input SOP is important to optimize this interaction.

The principle concept of a digital transfer function explains that an optical AND gate output AB power state depends on its input A and input B power state. An output AB power should have a high-state power when dual input A and input B pulses injected together into the FPSOA (input A and input B have a high-state power). Furthermore, an output AB power should have low-state power if at least one of the input signals has a low-state power.

5.1.2 The Basic Principle of Output SOP Alignment

We explore a new technique that takes advantage of having polarization diversity in the output AB SOP. This technique aims to align the output AB SOP to enhance the contrast of an optical AND gate toward 31.2 dB. This new technique has recently been employed to conduct all optical flip-flop operation [5].

Figure 5.1 illustrates a basic schematic diagram that explains the output AB SOP alignment process. The process of aligning the output AB SOP requires adding polarization controllers (PCs) after the FPSOA. Furthermore, this process requires

adding a linear polarizer to block the low-state power output AB for input case $A=1, B=0$, and passing the output AB of high-state power for input case $A=1, B=1$ through the polarizer.

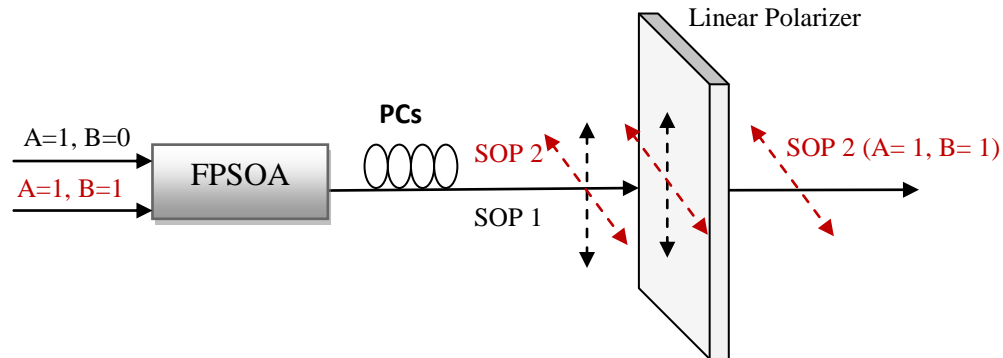


Figure 5.1: Output AB SOPs alignment for enhancing optical AND gate contrast.

For example, when the output AB for input $A=1, B=0$ has a distinct SOP 1, the role of PCs is to change the SOP until the polarizer blocks it. However, the polarizer will allow output AB for input case ($A=1, B=1$) to pass through it because output AB for high-state power undergoes polarization rotation that rotated output AB SOP 1 to SOP 2 as shown in Figure 4.2. In other words, introducing input B pulse signal into the FPSOA cavity for input case $A=1, B=1$ will rotate the output SOP from SOP 1 to SOP 2 via cross-polarization rotation (XPoIM; therefore, SOP 2 will partially pass through the polarizer.

5.2 Experimental Setup

The set values of input A and input B pulses (power, wavelength, and SOP) remained the same as in Chapter 4. Input A pulses have a 10 ns pulse width with a peak power of -18.7 dBm. This peak power includes the coupling loss of 9 dB between the fiber and FPSOA (fiber-to-SOA coupling loss). This peak power value is corresponding to 135-fJ pulse energy. The input A wavelength is 1604.042 nm.

The input B pulses have a 10 ns pulse width with a peak power of -22.2 dBm including the coupling loss of 9 dB between the fiber and FPSOA (fiber-to-SOA coupling loss). This means that input B pulse energy is 60-fJ. The input B wavelength is 1591.396 nm. Both input A and input B input power profiles are shown in Figure 3.5 in Chapter 3.

In terms of the input SOP alignment setting values, input B SOP is the TE mode while the input A SOP experiences polarization rotation. Polarization rotation is obtained when input A SOP is moved away from TE mode by using the PCs after MZM A as shown in Figure 5.2. These PCs rotated manually the orientation angle input A polarization angle by 54.1 degrees. A 54.1 degrees corresponds to 34.4% and 65.6% of input A power that injected into the FPSOA TE and TM modes, respectively, as explained in section 4.2 in Chapter 4.

In this chapter, a new experimental method is used to align the output AB SOP. Aligning the output AB SOP requires adding polarization controllers (PCs) in the output power path of the FPSOA. Furthermore, this process requires adding a linear polarizer as shown in Figure 5.2.

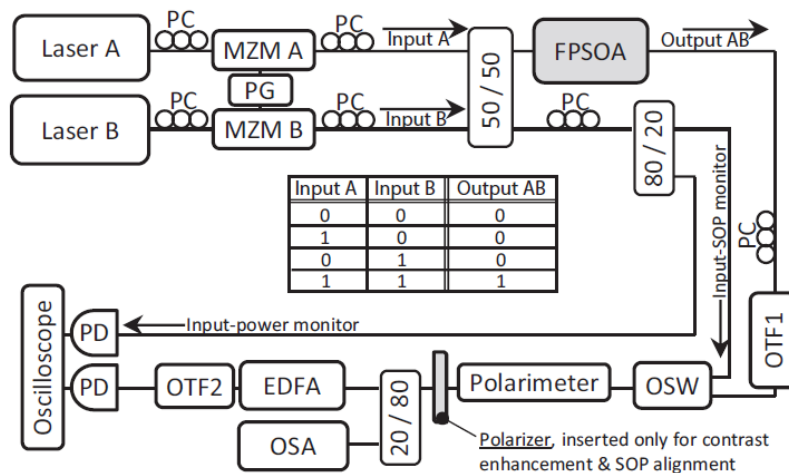


Figure 5.2: Experimental set up of an optical AND gate and output AB SOP alignment technique.

In Figure 5.2, the function of the PCs is to change the output AB SOP for the low power state orientation according to the blocking axis of a linear polarizer. The polarizer has an extinction ratio exceeding 40 dB. The purpose of using the in line polarizer is to block the output AB SOP for low power state of input case $A= 1, B= 0$.

Although the optical spectrum analyzer (OSA) was used to measure the output AB spectrum of the optical AND gate in previous chapters, the OSA is an essential diagnostic in this chapter to align the output AB SOP. Due to the SOA high sensitivity feature and ability of measure weak optical signals, the OSA device was used as a power monitoring device to align the output AB SOP. Furthermore, this device was used to measure the optical AND gate contrast in this experiment after completing the output AB SOP alignment procedures.

Chapter 5 conducts an optical AND gate by aligning the output AB SOPs that follows the experimental steps in Chapter 4.

The experimental procedures to align the output AB SOP are:

- After adding PCs and the linear polarizer as shown in Figure 5.2, the first step is working with the output AB of low state power for the input case $A= 1, B= 0$. This case has a unique SOP on the Poincare sphere as shown in Figure 4.3 in Chapter 4.
- The second step is setting the OSA functions to only track the peak power of output AB for input case $A= 1, B= 0$; the OSA requires specific settings to become more sensitive for tracking the output AB power as given below:
 - a) Set the OSA central wavelength as same as the central wavelength of the input A signal. This setting will make the OSA show the peak power of a solitary input A signal,

- b) set the OSA resolution to 0.02 nm,
 - c) set the OSA wavelength span function to zero nm (showing only input A peak power in the OSA trace). This setting will help to monitor only the peak power of input A,
 - d) set the OSA to experience a high sensitivity mode, and
 - e) set the OSA sweep function on repeat mode.
- Finally, while monitoring the output AB for the low state power on the OSA for the input signal A peak power, change the PCs after the FPSOA to obtain the optimum suppression of the output AB for signal A peak power in the OSA trace. Suppressing the output AB means forcing the output AB power [dBm] to experience the lowest possible power level when the solitary input A is injected into the FPSOA.
 - After completing the AB SOP alignment, the output AB for input A case $A=1, B=0$ forced to be orthogonal to the transmitting plane of the polarizer (aligned to propagate in the blocking axis of the polarizer). Thus, the polarizer blocks the output AB for low power state.
 - Reset the OSA functions such as wavelength span, sweep mode for the normal settings, and then capture the output AB spectrum of the optical AND gate for input case $A=1, B=0$.
 - Introduce the input B pulse into the FPSOA and capture the output AB spectrum for the input case $A=1, B=1$ without changing any setting values in this stage of the experimental procedure.

5.2.1 Optical AND gate via output AB SOP Alignment

When both input A and input B optical pulses enter the FPSOA, the output AB SOP rotates via XPolM. The output AB SOP depicted a 60.9 degree difference on the Poincare sphere between output AB SOP for the dual input case $A=1, B=1$ and the solitary the input A case $A=1, B=0$. A 60.9 degree corresponds to 33.8% orthogonality as explained in Figure 4.3 in Chapter 4.

Figure 5.3 shows the OSA spectrum for the solitary input A case $A=1, B=0$ before placing the polarizer. In addition, this figure shows the output AB for the solitary input A case $A=1, B=0$ after completing the output AB SOP alignment technique.

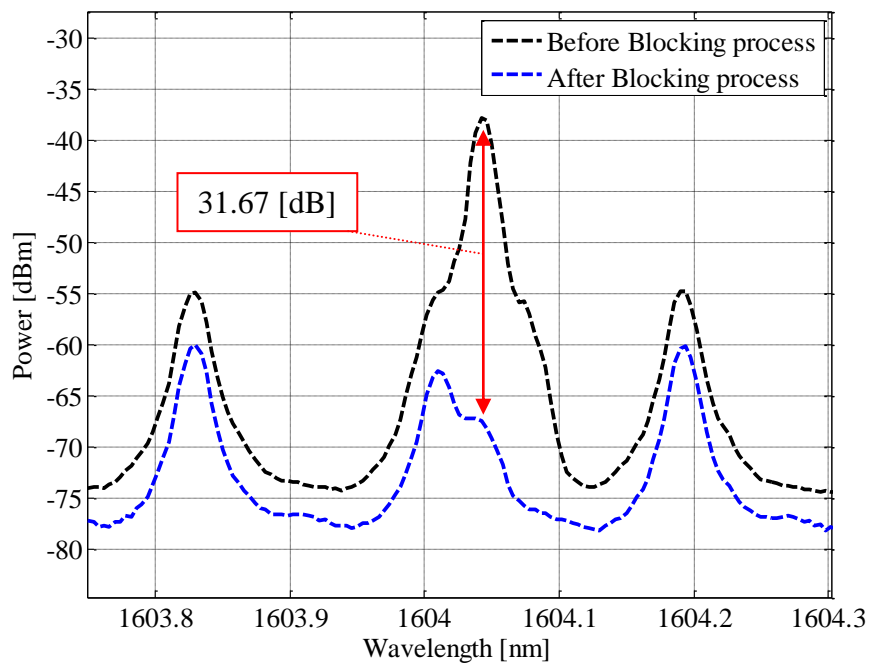


Figure 5.3: Output AB for input case $A=1, B=0$ before and after introducing the polarizer.

This figure shows that the output AB for the input case $A=1, B=0$ power is -35.76 dBm before introducing the polarizer. In addition, this figure shows the output AB for the same input case when introducing the polarizer. The polarizer suppressed the output AB power to an extremely low peak power of a -67.43 dBm.

However, this blocking process is not effective if output AB SOP changed. When input B is introduced into the FPSOA cavity, the output AB SOP rotates by XPolM by 60.9 degrees. This rotation is measured on the Poincare sphere of the polarimeter as shown in Figure 4.3 in Chapter 4. The polarization rotation allows the output AB of the input case $A=1, B=1$ to partially pass through the polarizer as shown in Figure 5.4.

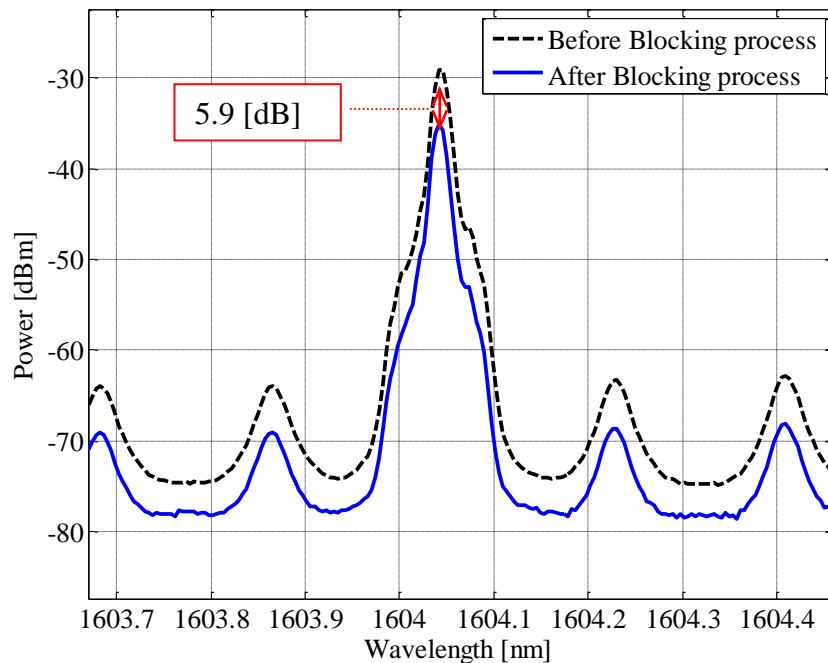


Figure 5.4: Output AB for input case $A=1, B=1$ before and after introducing the polarizer.

This figure shows the output AB peak power before and after introducing the polarizer for the input case $A=1, B=1$ in the OSA trace. Even if the polarizer is optimized to only block the output AB for the input case $A=1, B=0$, this figure shows that the output AB is dropped from -29.18 to -35.08 dBm due to several factors

such as the insertion loss of the polarizer and the SOP of output AB for the input case $A=1, B=1$. In other words, the output SOPs alignment technique is not used for optimizing the input case $A=1, B=1$ to pass through the polarizer.

Figure 5.5 (a) shows the output AB of the optical AND gate measured with an oscilloscope trace. This figure shows indiscernible power level for the output AB of a solitary A pulse ($A=1, B=0$) after using the output AB SOP alignment process. Furthermore, this figure shows the output AB power for the input case that partially passed through the polarizer ($A=1, B=1$).

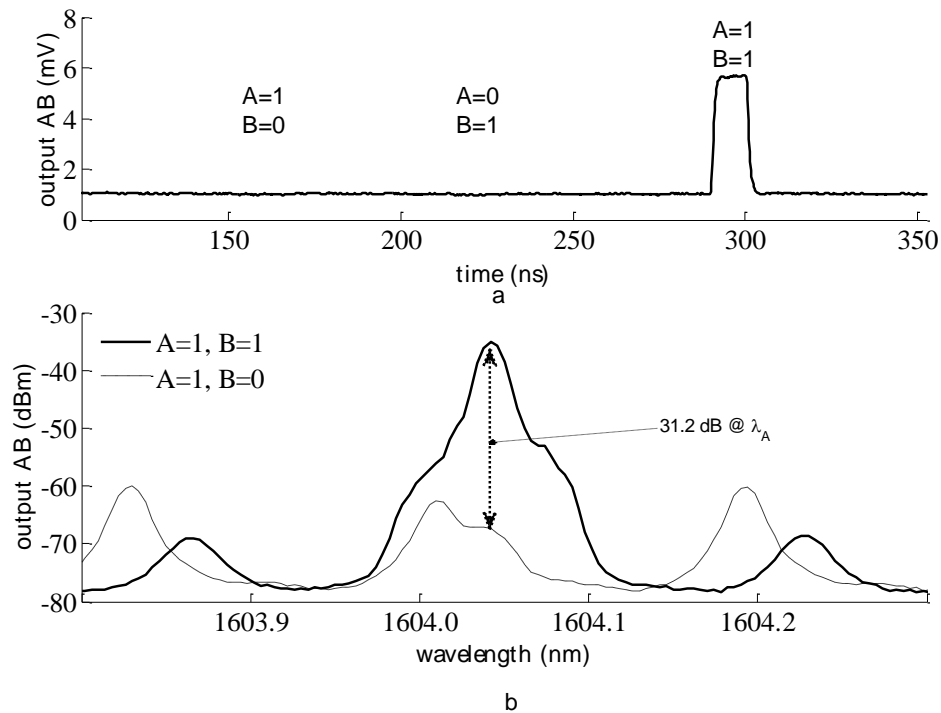


Figure 5.5: (a) Optical AB signal having an indiscernible level for solitary A pulse case (b) A contrast of 31.2 dB is measured using the OSA.

Furthermore, Figure 5.5 (b) reveals a 31.2 optical AND gate contrast measured by using the OSA. The OSA trace shows an extremely low power of input case $A=1, B=0$. An extremely low power is performed because the in-line polarizer blocked this signal. Introducing input B pulse shifted a FP resonance toward the input A central

wavelength via cross phase modulation (XPM). This FP resonance is optimized to place on top the input A signal.

In addition, the output AB SOP rotated due to XPolM when the input A signal undergoes polarization rotation. As a result of this rotation, the polarizer output will allow part of the output AB power of input case $A=1, B=1$ to pass through it.

The output AB of our optical AND gate in this experiment showed a typical optical AND gate functionality that has not shown in previous demonstrated data for such FPSOA device. In this finding, the output AB exhibits a high state power if both input A and input B optical pulses are injected together into the FPSOA. Hence, this new mechanism of aligning the input signals condition to experiences a polarization rotation and aligning the output AB SOPs of contrast enhancement technique produces a 31.2 dB contrast of the optical AND gate.

Chapter 6

Concluding Remarks

A 32.1dB optical AND gate contrast is demonstrated in this thesis based on cross polarization modulation (XPolM) within the resonance cavity of a Fabry-Pérot semiconductor optical amplifier (FPSOA). The optical AND gate functionality itself emerges from cross phase modulation (XPM) between the input signal and a FP resonance under controlled conditions. Both XPolM and XPM depend on such conditions as input power, wavelength, and state of the polarization (SOP).

Chapter 2 characterized the FPSOA resonance behavior due to XPM and cross gain modulation (XGM) with several series of experiments. Characterizing longitudinal modes of the FPSOA showed:

- The FPSOA is anisotropic in gain. The TE mode spectrum has a higher ratio of peak to valley height than the TM mode, revealing more gain for the TE mode than the TM mode.
- The FPSOA is a birefringent device due to a refractive index difference between the TE mode the TM mode. The FPSOA birefringence makes the TE and the TM resonances in phase or out of phase over the gain spectrum.
- Resonances shift to the long wavelength when input power enters the FPSOA cavity because the input power depletes the carrier density that leads to an increase in the refractive index. This is XPM.

- In addition, the peak power of resonances reduce when input power inject into the FPSOA due to the gain reduction. This is XGM.

Chapter 3 investigated the optical AND gate basic operation. The input A and input B SOP was aligned to the TE mode for $\rho=1$ [-]. An 8.5-dB contrast of the optical AND gate is measured. Cross phase modulation (XPM) is used to trigger the optical AND gate functionality.

In Chapter 4, Input A is forced to undergo polarization rotation by rotating its SOP to propagate into the two polarization modes of the FPSOA. Conducting optical AND gate operation along with polarization rotation showed:

- Rotation was achieved for the input A SOP for $\rho=0.3434$ [-]. The ρ value indicates that a 66 % of the total power injected into the TM mode while a 34 % input A remains of the total power injected into the TE mode of the FPSOA.
- The output AB SOP shows polarization diversity due to cross polarization modulation XPolM.
- XPolM rotates the output AB SOP when input B is introduced into the FPSOA (A= 1, B= 1).
- Rotation of the input A SOP showed 60.9 degrees separation between the output AB SOPs. In other words, the output AB SOP for inputs (A= 1, B= 0) is different from (A= 1, B= 1) cases.

Chapter 5 takes advantage of having polarization diversity in the optical AND gate output by aligning the output AB SOP to a linear polarizer. The polarizer is used to block the low-state power of the input case (A= 1, B= 0) that has a specific SOP. Then, when the output AB SOP is rotated due to XPolM for the input case (A= 1, B=

1), the power partially passes through the polarizer. In summary, this thesis shows a new technique of controlling the polarization sensitivity of the FPSOA to improve the optical AND gate contrast by 24 dB more than previous demonstrations for FPSOA devices.

Bibliography

- [1] Willner, Alan E., et al. "All-optical signal processing." *Lightwave Technology, Journal of* 32.4 (2014): 660-680.
- [2] Scaffardi, Mirco, et al. "Photonic processing for digital comparison and full addition based on semiconductor optical amplifiers." *Selected Topics in Quantum Electronics, IEEE Journal of* 14.3 (2008): 826-833.
- [3] Sharfin, W. F., and M. Dagenais. "High contrast, 1.3 μm optical AND gate with gain." *Applied Physics Letters* 48.22 (1986): 1510-1512.
- [4] Guo, Li-Qiang, and Michael J. Connelly. "All-optical AND gate with improved extinction ratio using signal induced nonlinearities in a bulk semiconductor optical amplifier." *Optics Express* 14.7 (2006): 2938-2943.
- [5] Ippolito, C. E., et al. "All-optical flip-flop contrast enhancement based on bistable polarisation rotation within Fabry–Perot SOA." *Electronics Letters* 50.22 (2014): 1620-1622.
- [6] Ma, B., M. Saitoh, and Y. Nakano. "All-optical wavelength conversion based on Fabry-Perot semiconductor optical amplifier." *Lasers and Electro-Optics, 2000.(CLEO 2000). Conference on. IEEE, 2000.*
- [7] Connelly MJ, Ebrary I. *Semiconductor optical amplifiers*. Boston: Kluwer Academic Publishers; 2002;2007;2001;.
- [8] Venghaus H, Grote N, SpringerLink. *Fibre optic communication: key devices*. New York; Berlin;: Springer; 2012.
- [9] Agrawal, Govind P. *Nonlinear fiber optics*. Academic press, 2007.

- [10] Soto, H., D. Erasme, and G. Guekos. "Cross-polarization modulation in semiconductor optical amplifiers." *Photonics Technology Letters, IEEE* 11.8 (1999): 970-972.
- [11] Keiser G. *Optical fiber communications*. 5th ed. New York, NY: McGraw-Hill Companies; 2013.
- [12] Kumar, Arun, and Ajoy K. Ghatak. "Polarization of light with applications in optical fibers". Vol. 246. SPIE Press, 2011.
- [13] Fu, Songnian, et al. "Nonlinear polarization rotation in semiconductor optical amplifiers with linear polarization maintenance." *Photonics Technology Letters, IEEE* 19.23 (2007): 1931-1933.
- [14] Wen, Pengyue, et al. "Vertical-cavity optical AND gate." *Optics communications* 219.1 (2003): 383-387.
- [15] Maywar, Drew N., Govind P. Agrawal, and Yoshiaki Nakano. "All-optical hysteresis control by means of cross-phase modulation in semiconductor optical amplifiers." *Journal of the Optical Society of America B* 18.7 (2001): 1003-1013.
- [16] Bhargava, Swati, et al. "Optical bistability in a nonlinear resonance with saturable losses and intensity-dependent refractive index." *Communications (ICC), 2010 IEEE International Conference on*. IEEE, 2010.